AN INVESTIGATION TO SIMULATE THE LINEAR VISCOELASTIC BEHAVIOR OF AN ELASTOMER

RICHARD L. CITERLEY

AN INVESTIGATION TO SIMULATE THE LINEAR VISCOELASTIC BEHAVIOR OF AN ELASTOMER

****

Richard L. Citerley

AN INVESTIGATION TO SIMULATE THE LINEAR VISCOELASTIC BEHAVIOR OF AN ELASTOMER

by

Richard L. Citerley
Instructor, Department of Aeronautics
United States Naval Postgraduate School

Submitted in partial fulfillment of
the requirements for the degree of

MASTER OF SCIENCE

IN

MECHANICAL ENGINEERING

United States Naval Postgraduate School
Monterey, California
1961

AN INVESTIGATION TO SIMULATE THE LINEAR VISCOELASTIC BEHAVIOR OF AN ELASTOMER

by

Richard L. Citerley

This work is accepted as fulfilling
the thesis requirements for the degree of
MASTER OF SCIENCE
IN
MECHANICAL ENGINEERING
from the
United States Naval Postgraduate School

ABSTRACT

For vibration and shock isolation investigations the conventional engineering representation of an elastomer under shear is a mechanical model with a spring and a dashpot in parallel. To represent more adequately the dynamic behavior of an elastomer, more complex model configurations are required. The technique to determine and assign magnitudes of a particular model configuration is presented. With the aid of an electronic analog computer, the frequency response characteristics of a particular elastomer are verified and the shock response characteristics are then predicted. The results obtained by this technique indicate an excellent correlation of behavior between the assumed model representation and the elastomer.

ACKNOWLEDGEMENTS

The writer wishes to express his appreciation to Mr. J. A. Townsend, Firestone Tire and Rubber Company, for the elastomer used in this investigation, to Mr. Kenneth Mothersell for his assistance in fabricating and machining the test equipment, to Mrs. Margenette Kirkman in preparing the manuscript, and to Professors Robert E. Newton and George J. Thaler of the U. S. Naval Postgraduate School for their assistance and encouragement in this investigation.

TABLE OF CONTENTS

LIST OF ILLUSTRATIONS

LIST OF SYMBOLS

Symbol	Description	Units
A	Area	$in.^2$
c	Damping Coefficient	lb-sec/in.
C	Capacitance	farads
E	Modulus of Elasticity	$lb/in.^2$
f	Frequency	cycles/sec
F, P	Force	lbs
h	Thickness of Ring Cross-section	in.
G	Shear Modulus	$lb/in.^2$
I	Second Moment of Area	$in.^4$
K, k	Spring Constant	lb/in.
m, M	Mass	$lb\text{-}sec^2/in.$
M	Moment	in-lb
R	Resistance	ohms
R_t	Radius	in.
T	Shear Pad Thickness	in.
t	Time	sec
V, e	Voltage	volts
δ, y, x, u, v, w	Displacement	in.
ϵ	Tensile Strain	in./in.
γ, $\S$	Shear Strain	rad
ϕ	Phase Angle	rad
η	Viscosity	$lb\text{-}sec/in.^2$
σ	Shear Stress	$lb/in.^2$
τ	Relaxation Time	sec
ω	Circular Frequency	rad/sec
ω_b	Circular Frequency of Calibration Beam	rad/sec
ω_t	Circular Frequency of Transducer	rad/sec

Chapter I

INTRODUCTION

The problem considered is that of the determination of the dynamic response characteristics of an elastomer under shear. The object of the investigation is to determine a mathematical model which is the mechanical analog for the linear viscoelastic behavior of an elastomer. The frequency range under consideration is limited to two decades--1 to 100 cps. Within this range, the dynamic behavior of an elastomer is measured and then simulated by an electronic analog computer. Once an agreement exists between simulated and measured results, the shock response of an elastomer is predicted. This prediction, again performed by an analog computer, is compared to values experimentally obtained.

This type of investigation is of interest because elastomers of all shapes, stiffness and damping properties are commonly used for vibration isolation and shock mitigation.

The mechanical properties of most elastomers are known to be nonlinear. Some attempts have been made to represent these characteristics by analytical methods.[1] If the linear characteristics are of interest, the classical single Voigt[2] (Fig. 1) mechanical unit (dashpot and spring in parallel attached to a massless beam) is generally assumed. The linear spring supplies a force that is proportional to displacement, and the dashpot supplies a force that is proportional to velocity. If this model is assumed to represent the dynamic behavior of the elastomer, a discontinuity in force as a function of time would exist for a forcing function having the character of a finite velocity step. For most elastomers, the above phenomenon is not observed.

For many engineering investigations, the single Voigt unit is generally assumed to be adequate to describe the behavior of

elastomers under shear. If, however, the shock behavior or time dependent properties of an elastomer (e.g., stress relaxation or dynamic stiffness) are of interest, a single Voigt unit appears to be inadequate to represent these phenomena.

The dynamic response characteristics of a single Voigt unit have been compared to those of other mechanical models[3-8, 14, 17] R. E. Newton and L. E. Matthews[3] present a comparison of shock behavior of a single Voigt unit to that of a number of Maxwell units in parallel.[4] A Maxwell unit consists of a spring and dashpot in series (Fig. 2). T. Alfrey[5], B. Gross[6], W. Kuhn[7] and R. Tuckett[8] have compared the interrelationships between a number of Voigt units in series (Fig. 3) and a number of Maxwell units in parallel (Fig. 4) to represent the analogous shock and dynamic response characteristics of an elastomer.

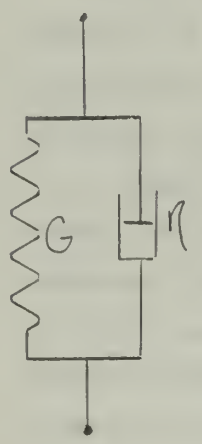

Fig. 1
Voigt Unit

Fig. 2
Maxwell Unit

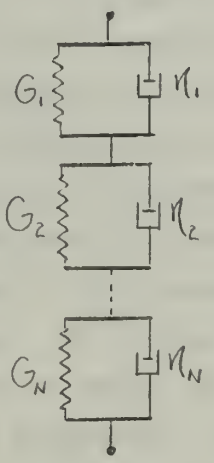

Fig. 3
Voigt Model

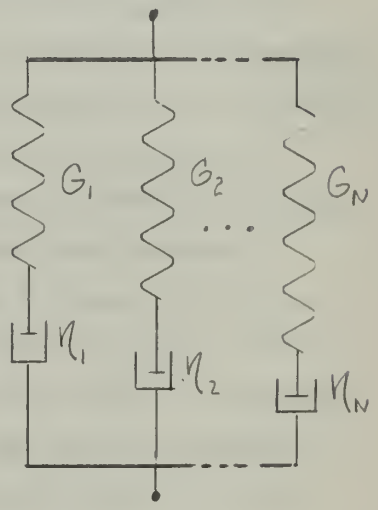

Fig. 4
Maxwell Model

Most of the works cited show the general analytic behavior of an elastomer under shear for an infinite frequency or time spectrum. The actual reduction procedure of the appropriate data for a particular frequency range, or the selection procedure

of the number and arrangement of the mechanical units previously outlined, have not been conveniently described.

Experimental procedures to evaluate the dynamic behavior of an elastomer can be subdivided into two categories: transient investigations and steady state forcing frequency investigations. For transient investigations, R. S. Stein and A. V. Tobolsky[9] developed an apparatus to measure shearing strain for a known shearing stress. By adjusting a weight, constant strain was maintained over a period of time in excess of 100 hours. From these measurements, the remaining dynamic characteristics can be predicted[5-9]. The accuracy requirements on the measuring elements demand close tolerance equipment. Not only is precise and costly measuring equipment required, but the test cannot be interrupted.

The most popular method of experimentally determinimg the behavior of an elastomer is under a forcing sinusoidal displacement. Many devices, such as electromagnetic drives used by R. B. Blizard[11], and added inertial resonance devices used by J. H. Dillon and S. D. Gehman[12], provide in-phase and quadrature stiffness measurements. By subjecting the elastomer to a known displacement, a resultant force can be measured. This force is directly related to the stress in the elastomer. By varying the frequency of the (simple harmonic) displacement, a survey of the dynamic characteristics of an elastomer can be performed. This general method is used for this investigation. The equipment description and the necessary experimental technique to assign and evaluate the parameters in convenient form are established in Chapter III.

The frequency range of a sinusoidal displacement device has some upper limit, J. D. Ferry[13] proposed that under controlled temperature conditions the dynamic behavior of an elastomer can be predicted for frequencies well beyond the frequency limitations of the experimental apparatus.

Assuming that either a number of Voigt or Maxwell units closely represent the dynamic behavior of an elastomer, the principal applicable relationships are described in Chapter 2. In addition, a description of the experimental equipment and procedure for evaluating the shock and vibration response characteristics of a particular elastomer by electronic analog computer is also presented.

Chapter II

DISCUSSION OF THE APPLICABLE THEORIES AND THEIR LIMITATIONS

A linear viscoelastic material has been defined[5] as

> ...one which, under stress gives a response that is a combination of linear elastic and linear viscous behavior.

Many elastomers have these properties. In order to duplicate the observed time dependence (as a result of viscous effects), mechanical models are assumed. Representing the viscoelastic material by some mechanical model does not imply that the molecular structure of the material is arranged in a similar manner. It is implied however, that some substance or combination of substances provides a characteristic reaction that can be duplicated by a particular mechanical element. For example, the sulphur content of a number of cross-linked high polymers provides damping. The damping for a mechanical model is represented by a dashpot.

To duplicate the overall elasticity of an elastomer, a spring element must be provided. Because the elasticity is dependent on frequency, an additional spring in series with a dashpot must be provided. For many cross-linked high polymers the amount of carbon black determines the magnitude of the spring constant associated with the observed linear elasticity.[15]

If one is to consider the study of the viscoelastic behavior of an elastomer and wishes to describe the dynamic response with a few mechanical units, the type of polymer must be considered. For example, non-cross-linked polymers have the characteristic of showing a permanent set after the release of an applied load. Moreover, the amount of permanent set is dependent on the magnitude of the applied load, the time that the load was applied and subsequently released, and the viscosity (sulphur content).

To duplicate this phenomenon with a mechanical model, one of the elements of the Voigt model must be a single dashpot, or all of the spring elements in the Maxwell model must have dashpots in series with their respective springs. For a cross-linked polymer, the model representation must again be slightly modified. One of the units for either the Voigt or Maxwell models must have a dashpot eliminated.

When dealing with the vibration characteristics of rigid bodies, the spring and dashpot arrangements of an assumed mechanical model are normally assigned the parameters of a spring constant k(lb/in), and a damping constant c(lb-sec/in). For viscoelastic investigations, when dealing with the mechanical properties of an elastomer, it is more convenient to refer to shear modulus, $G(lb/in.^2)$, for the spring and viscosity, η $(lb\text{-}sec/in.^2)$, for the dashpot. With this adoption in nomenclature, the shear behavior of the elastomer can be expressed independent of the specimen configuration. This will hold true when the results of the investigation are expressed in terms of shearing stress, σ $(lb/in.^2)$, rather than force, and shearing strain, γ (rad), rather than displacement. Knowing the cross sectional area and the thickness of the shear specimen that is used as a shock or vibration isolator for a particular rigid body, the motion of the body can then be determined.

From strength of materials concepts, the shear stress in a body is related to shear strain by a constant of proportionality, G. Since the two time dependent functions, stress and strain, may have some phase angle between them, it is convenient to specify the shear modulus in terms of components.

If the shear strain is a sinusoidal function of time with circular frequency ω, the shear stress and shear strain can be represented

by vectors rotating at angular velocity ω (Fig. 5). For a known strain, a shear modulus component in phase with the strain can also be represented by a vector and is called the storage modulus G'. At 90^{o} to the strain, another shear modulus component can be represented by a vector and is called the loss modulus G".

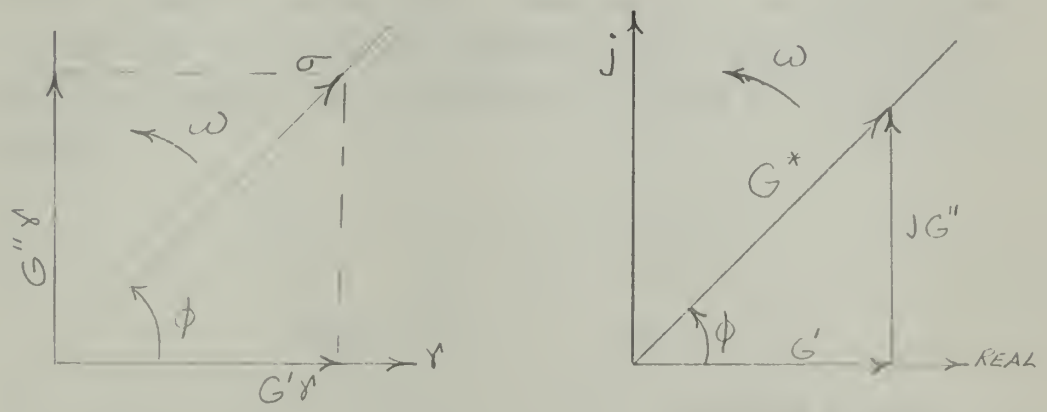

Fig. 5. Diagrams illustrating complex modulus and its components G', G"

Since these moduli are perpendicular to each other, they are also components of a complex shear modulus, G* (Fig. 5). If the complex notation is used, the components G' and G" are related to the complex modulus by the equation:

$$G^{*} = G' + jG'' \qquad 2.1$$

If the notation is other than complex, a dynamic modulus G is defined by the ratio of the stress amplitude, σ_a, to the strain amplitude, γ_a:

$$G = \frac{\sigma_a}{\gamma_a} \qquad 2.2$$

or

$$G = |G^{*}| = \left\{ \left[G'\right]^2 + \left[G''\right]^2 \right\}^{1/2} \qquad 2.3$$

The relationship between stress and strain for the Maxwell unit is given by the differential equation:

$$\dot{\sigma} + \frac{1}{\tilde{\tau}}\sigma = G\dot{\gamma} \qquad 2.4$$

where $\tau = \eta/G$

If one assumes a number (N) of these units in parallel, it can be seen that each unit will experience the same total strain. The above equation can be modified to include all units of the model:

$$\dot{\sigma}_i + \frac{1}{\tilde{\tau}_i}\sigma_i = G_i\dot{\gamma} \qquad 2.5$$

where i = 1, 2, ..., N.

For a known stress function, it is more convenient to use a Voigt model. The relationship between stress and strain for the Voigt unit is given by the differential equation:

$$\tau\dot{\gamma} + \gamma = \frac{\sigma}{G} \qquad 2.6$$

If one assumes a number (N) of these units in series, it can be seen that each unit must experience the same stress. The above equation can be modified to include all units:

$$\tilde{\tau}_i\dot{\gamma}_i + \gamma_i = \frac{\sigma}{G_i} \qquad 2.7$$

where 1 = 1, 2, ..., N.

To determine what type of test should be used, the characteristics of the above equation as applied to an assumed model are now considered. If a stress, applied suddenly and then held constant, is imposed on an elastomer and the resultant strain-time history of the elastomer is recorded, a transient phenomenon called creep can be observed. It can be shown that creep data can be

used to predict other dynamic response characteristics.[18] The problem confronted in this type of experimental investigation is that, for predicting the shock response of an elastomer, the material properties that are of major interest are not easily experimentally accesible when the time scale of the strain-time history is small compared to the time of application of the stress.

Another transient experiment that could be considered is stress relaxation. For this case, a strain suddenly applied and then held constant is imposed on an elastomer and the stress-time history is recorded. Again, the material properties that are applicable in predicting the shock response of an elastomer can not be easily measured. It is very difficult to provide a forcing function for either of the above test procedures that has a sufficiently small rise time to measure the desired properties.

To predict the shock behavior of an elastomer from dynamic measurements, it is generally easier to measure the frequency response characteristics of an elastomer under sinusoidal excitation in the desired frequency range. At a particular frequency of sinusoidal displacement, the dynamic properties of the elastomer can be measured repeatedly. In addition, these properties can be measured at the desired time interval. A number of discrete frequencies can be selected and a range of response characteristics is determined. This procedure was therefore chosen as the experimental procedure.

Since an eccentric displacement of a rotating cam or connecting rod and crank is much easier to obtain than a prescribed varying force, the Maxwell model representation (Fig. 6) is used for this investigation.

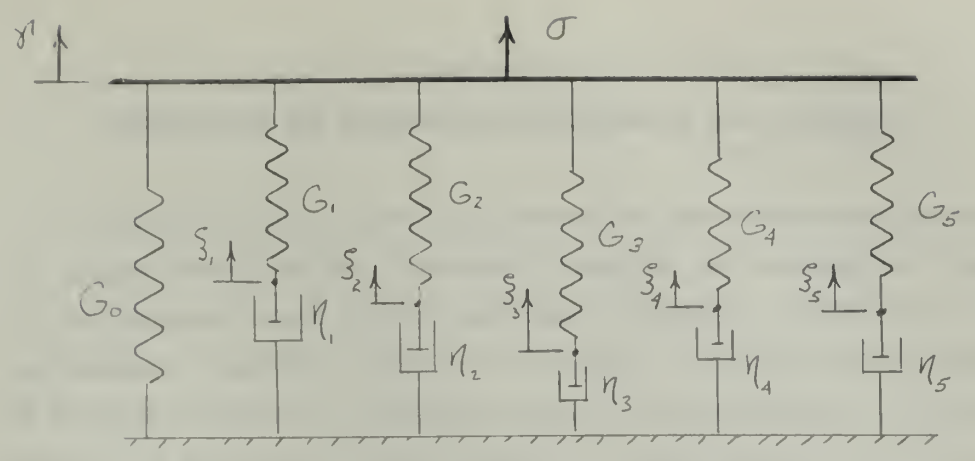

Fig. 6. Maxwell model for SBR elastomer

For a known sinusoidal forcing strain, $\gamma' = \gamma'_o \sin \omega t$, the in-phase (storage) modulus G' and the quadrature (loss) modulus G" are given by Eqs. A-14, A-15 and A-16:

$$G' = G_o + \sum_{i=1}^{i=N} G_i \frac{(\tau_i \omega)^2}{1 + (\tau_i \omega)^2} \qquad 2.8$$

$$G'' = \sum_{i=1}^{i=N} G_i \frac{(\tau_i \omega)}{1 + (\tau_i \omega)^2} \qquad 2.9$$

A factor $\tau_i = \eta_i / G_i$ is associated with each Maxwell unit. This factor is sometimes referred to as the relaxation time constant of the Maxwell unit and has the dimensions of time. The reciprocal of the time constant corresponds to a characteristic circular frequency. At this frequency, the quadrature (loss) component of the dynamic modulus is at its maximum. A more detailed discussion on the development of the above equations is given in Appendix A.

Chapter III

DESCRIPTION OF EXPERIMENTAL EQUIPMENT AND PROCEDURE

The selection of test equipment and the associated instrumentation is largely based on the frequency range to be considered. Since most of the commonly used rotary electrical devices operate at an approximate frequency range of 30-60cps, it would be desirable to know the vibration characteristics of an elastomer in this range. In addition, since industrial road equipment, missiles and other large bodies have natural frequencies in the order of 3-5 cps, it would be equally desirable to investigate this range in frequency. Accordingly, a two decade frequency range of 1 to 100 cps is chosen.

As stated in Chapter II, the selected method of investigation requires that the specimen be given a sinusoidal displacement. An electric motor with suitable attachments can provide such a sinusoidal displacement. The design of the mechanical adapters and attachments should provide an approximate sinusoidal motion with the least complexity. Since most available electrical motors are of the squirrel cage type and have one synchronous speed, it is desirable to provide a variable speed transmission unit to have the capability of varying the frequency of the input displacements of the elastomer. In addition, to insure that no random acceleration or displacement inputs are delivered to the test specimen, either by direct or indirect means, the drive mechanism should be mounted separately from the specimen.

The upper frequency limit of the variable speed drive unit used is approximately 30 cps. Therefore, to investigate up to 100 cps, a higher frequency range machine is required. An electrodynamic shaker has this capability. Also, this machine is capable of producing sinusoidal frequencies within the upper range of the previously mentioned drive unit; therefore, an overlap in data will insure a smooth transition in test procedure.

The size of the specimen is based on several factors. The first is to insure a state of pure shear and to insure stability of an elastomer shear pad. To do this, a ratio of width or length to thickness should be at least four. The second factor is that the shear strain applied must be small. Since most elastomers are nonlinear for shear strains above 0.30 radians, the maximum sinusoidal displacement amplitude is maintained below 6% of the shear pad thickness, which corresponds to a shear strain below 0.06 radians.

The requirement that dictates the minimum size of the shear specimen is the backlash of the mechanical drive system. Since small strains are to be considered, the connectors and adapters from the drive system must have a minimum of backlash. If the input displacement is too small, the tolerances on the drive mechanism become more critical. The force transducer design also has a direct bearing on the acceptable force level. The force transducer must be a relatively rigid member so that deflection is small compared to the displacement of the specimen. If, however, it is made too rigid, low stress levels will be encountered and may be difficult to measure. With all these factors taken into account, a specimen size of ½" x 1" x 1" was selected.

The most commonly used elastomer for vibration and shock isolation is a tread stock rubber designated SBR (formerly GRS). This elastomer is used for this investigation. Since the dynamic modulus for SBR is low (the static shear modulus is approximately 100 $lb/in.^2$, corresponding to a Shore Durometer Number of 56), the force level and, in turn, the power requirements of the drive unit are quite low.

The force that the transducer measures has some phase angle relative to the applied sinusoidal displacement. The quadrature component of this force is a direct measure of the power or heat generated within the elastomer. From an approximate heat transfer evaluation, the maximum steady state temperature rise of the elastomer is estimated as $7^{o}F$. Since this value is low and since the laboratory temperature is maintained at approximately $70^{o}F$, the test results are considered to be independent of temperature effects.

Low Frequency Test Equipment

The mechanical arrangement used for determining the low frequency response of the specimen consists of a drive unit, power transmission, eccentric, connecting rod, specimen holder, connector plate, transducer and supporting platforms (Fig. 7). The source of power is ½ hp electric motor rated at 1750 rpm. Connected to the motor, through a flexible coupling, is a 3/4 hp hydraulic variable speed transmission rated 40 in-lb of torque at 1800 rpm. The motor and transmission are mounted on an 18" I-beam. The I-beam in turn is mounted on an adjustable work table.

The output shaft of the transmission unit is connected through another flexible coupling to an assembly consisting of an eccentric mounted at the end of a 3/4 inch diameter shaft that is supported by self-aligning bearing blocks. The eccentric throw has a range from 0.001 in. to 0.500 in. At the end of the eccentric a connecting rod and its bearing are attached. The eccentric bearing blocks and specimen holder are mounted on a base plate isolated from the drive support.

The six-inch connecting rod is in a plane perpendicular to the axis of the eccentric and in line with the specimen holder. Since the height of the center line of the specimen and eccentric axis are the same, nearly sinusoidal motion is transmitted to the specimen.

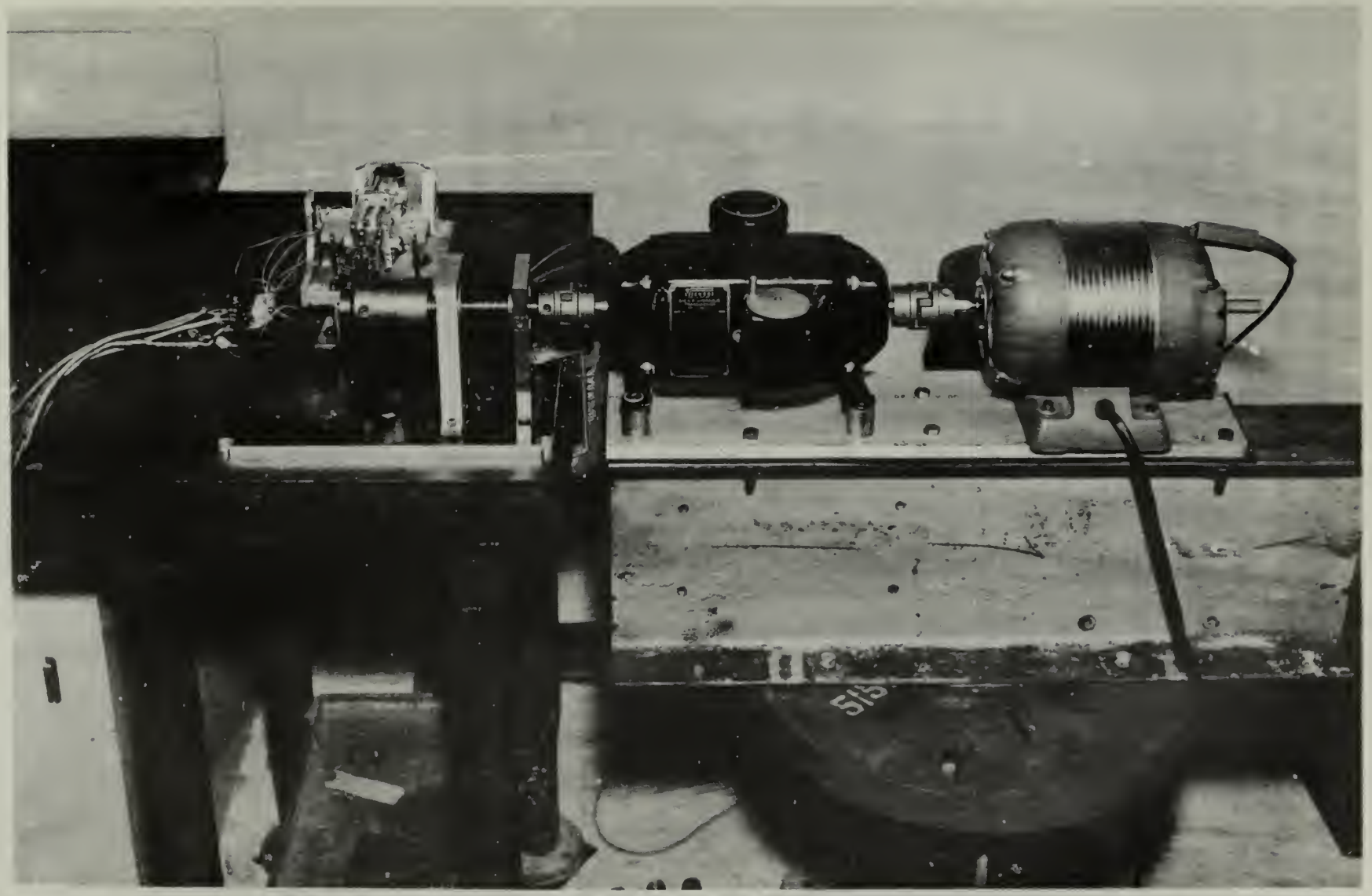

Fig. 7. Test Equipment for Low Frequency Investigations

At the end of the connecting rod an elastic hinge is present to insure that no moment is transmitted to the specimen. A set of leaf springs cantilevered from the base plate to the specimen holder enforce translation of the latter.

The specimen connector plate (previously described) is attached to the force transducer. The force transducer in turn is attached by a bracket to the base plate. A separate bracket mounted on the side of the base plate provides support for the displacement transducer which monitors the input displacement of the specimen holder.

Thus, sinusoidal motion is provided to the specimen, causing a shear strain in the elastomer. The resultant force is measured by the force transducer.

High Frequency Test Equipment

For high frequency investigation a 40 watt electrodynamic shaker is used for the drive (Fig. 8). The specimen holder and base plate are supported by a 10" channel attached to the top of the shaker. Sinusoidal motion is provided through a resonant beam which is excited by the shaker. A small adapter is provided to attach the beam to an elastic hinge. The force and displacement measurements are made in the same manner as in the low frequency tests.

Shock Response Test Equipment

The mechanical arrangement for shock response investigation uses the same base plate and specimen holder as the high frequency response investigation. The small adapter plate described above is used as the striker plate. To produce the shock, a pendulum with a 100 lb weight is used to strike the adapter plate.

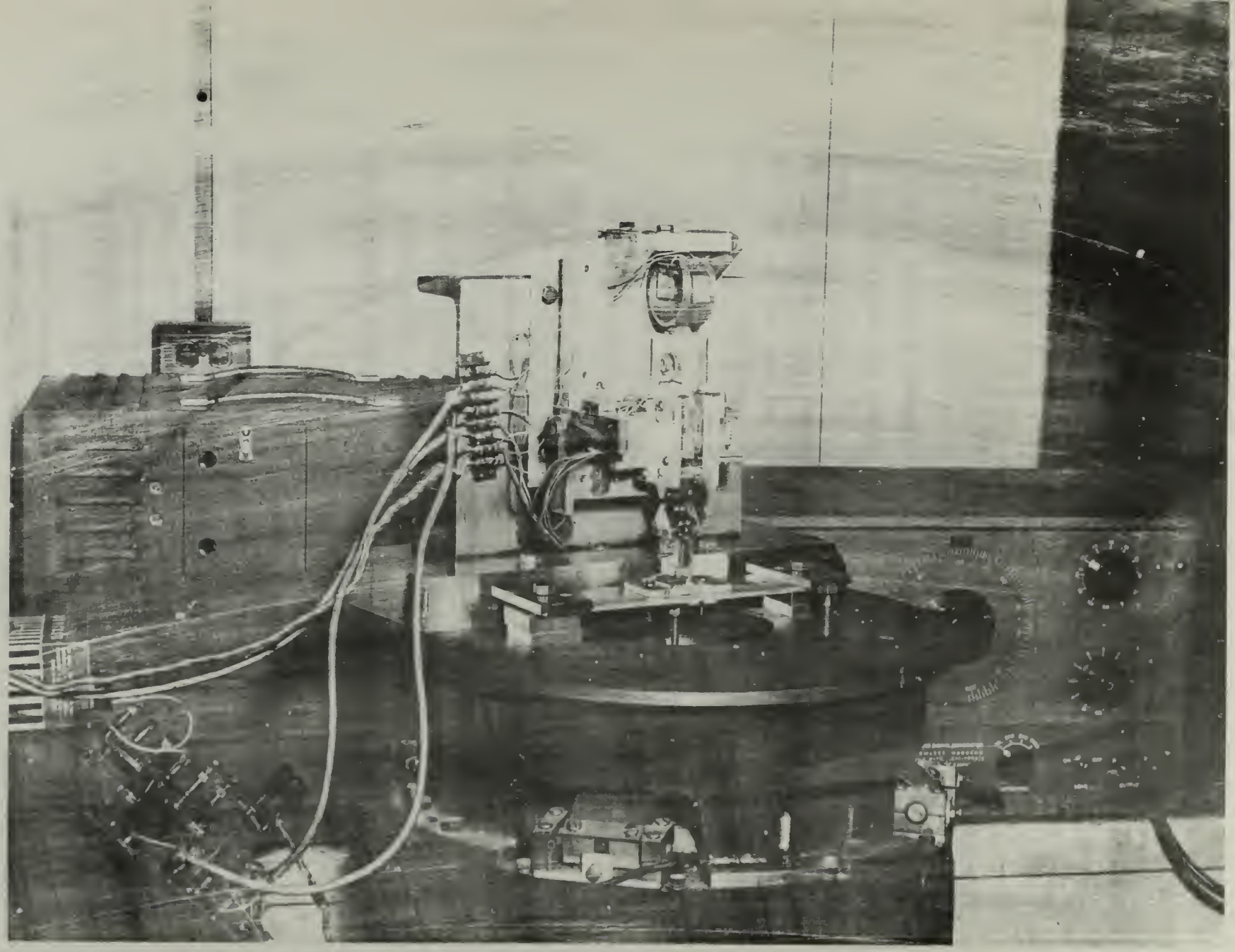

Fig. 8. Test Equipment for High Frequency Investigations

Transducers

As noted above, two transducers are used. One transducer measures the force transmitted by the elastomer shear pad and the second monitors the displacement of the specimen holder.

The force transducer is a steel ring. Mounted diametrically opposite and perpendicular to the applied force axis on the ring are four Bakelite flats, with a strain gage on each one. The displacement transducer is a cantilever beam with two resistance strain gages mounted near the root of the beam A more detailed description of the two transducers appears in Appendix B.

Instrumentation

The instrumentation for all frequency response investigations consists of an oscilloscope (with Polaroid camera attachment), amplifiers, and low pass filters. The output signal from the force transducer is amplified approximately 200 times, passed through a low-pass filter circuit (Fig. 9) to remove high frequency noise, and then applied to the vertical plates of the oscilloscope. Likewise, the output signal from the displacement transducer is amplified, filtered, and then applied to the horizontal plates of the oscilloscope. The resultant trace is a Lissajous figure in the form of an ellipse.

To conduct the low frequency investigation, the output signal of the force transducer is amplified by a Heiland carrier amplifier for the frequency range of 1 to 5 cps and an Ellis BA-2 bridge and amplifier is used for frequencies above 5 cps. Originally, a high bridge voltage was deemed necessary to record the resulting strain from the force transducer. Because the maximum allowable bridge voltage for the Heiland amplifier is 5 volts, the Ellis amplifier was considered for frequencies above 5 cps.

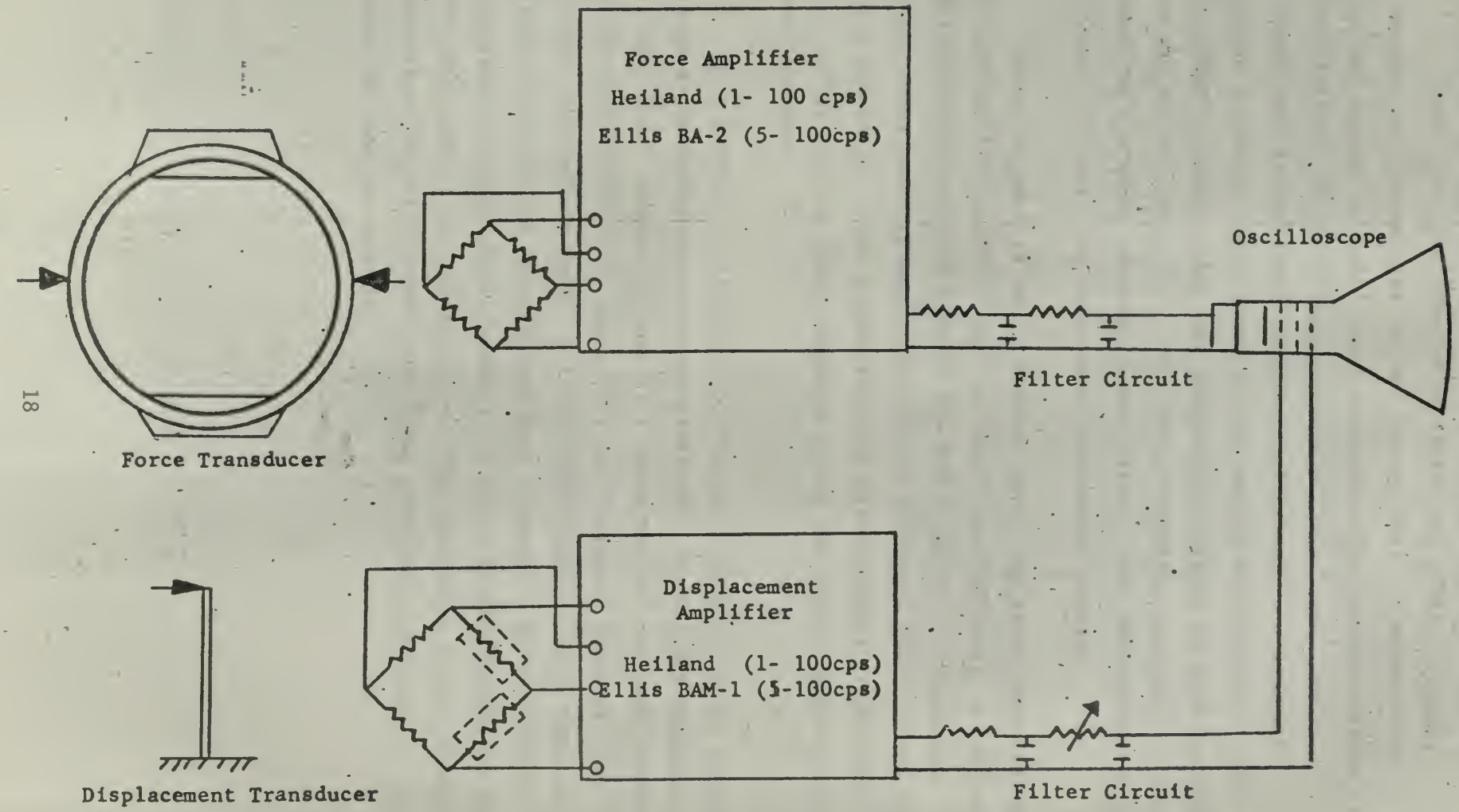

FIGURE 9.
INSTRUMENTATION CIRCUIT DIAGRAM

The Ellis amplifier has a flat frequency response from 5 to 25,000 cps. The Heiland amplifier has a flat frequency response for frequencies below 5 cps as well. Therefore the Heiland system was mainly used to measure the characteristics of the elastomer in the frequency range of 1 to 5 cps. As it turned out, the Heiland system was later used as a separate source to verify the results for the entire investigation. As a matter of convenience, the displacement signal is also amplified by the Heiland amplifier. This instrumentation procedure is also used for the shock response investigation. The Heiland Visicorder is used to record the force and displacement signals.

When the BA-2 is used, an Ellis BAM-1 amplifier and meter unit is used as the amplifier for the displacement signal. A low pass filter circuit is used between the BAM-1 and the oscilloscope. This filter characteristic is slightly different than the one used with the BA-2. A one megohm variable potentiometer is provided to correct for any phase mismatch of the two input signals to the oscilloscope.

As a further verification of the test results for the frequency response characteristics of the elastomer, the Heiland amplifier is used for a frequency range of 1-30cps and for the high frequency investigation (20 - 100 cps). For the frequency range of 1 to 30 cps, filter circuits are used. For the high frequency investigation, the filter circuits are removed from both channels. Since a slight variation in phase exists between the force channel amplifier and the displacement channel amplifier, the capacitive bridge balance circuit of the displacement amplifier provides correction of the phase for the two signals.

Experimental Procedure

The following experimental procedure applies to the low frequency investigation. With the specimen in its holder, an eccentricity of approximately 0.015 inches is adjusted on the eccentric cam and measured by a dial indicator. This eccentricity is approximately 6% of the pad thickness The electric drive motor is then turned on and through the variable speed transmission the frequency range from one to 30 cps is surveyed During the survey the displacement of the specimen holder is checked by a toolmaker's microscope to insure that the displacement amplitude remains constant.

With the drive motor turned off, the instrumentation equipment is turned on and allowed to warm up. The calibration of the equipment is checked by applying a calibration signal from the Ellis BA-2 amplifier to the vertical plates of the oscilloscope. If a deviation exists between the double amplitude of the resulting trace and a predetermined calibration height, the vernier vertical gain adjustment on the oscilloscope is adjusted and subsequently held constant.

After calibration, a frequency is selected; the drive motor is turned on; the transmission unit is adjusted and its output speed is verified by a tachometer. Once the frequency is set and the drive motor is turned off, the elastomer is locked-out. That is, the specimen holder and connector plate are bolted together so that the specimen experiences no shearing strains. The drive motor is again turned on and the one megohm potentiometer in the horizontal sweep filter circuit is adjusted until the oscilloscope trace degenerates to a straight line (Fig.10). Thus the input signals are in phase.

After the drive motor is turned off, the elastomer is released from the locked-out position. The drive motor is then turned on and

Fig.10. Lissajous Figure of Trace with Zero Phase Angle.

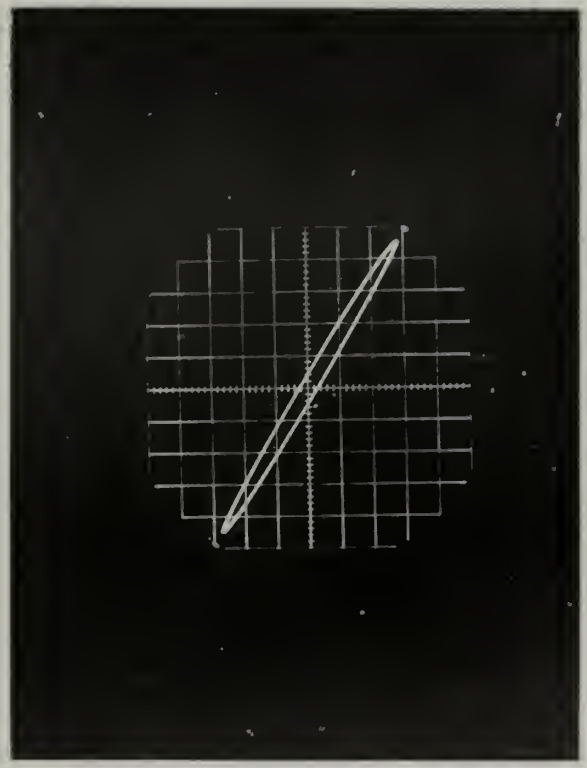

Fig. 11. Sample Data for Complex Modulus Measurements

the resultant elliptical figure is recorded on Polaroid film. The vertical gain position setting is also recorded. At each frequency selected, the procedure of displacement and frequency check, phase angle adjustment, and recording the data on film is repeated. To insure that the shear strain remains within the linear range of the elastomer, results are obtained for several different input displacements at each frequency.

For the high frequency runs, an electrodynamic shaker serves as the drive unit. The experimental procedure parallels that for the low frequency runs, but the displacement is set by adjusting the amplitude of the audio oscillator signal which controls the shaker amplifier. The displacement is again checked by a microscope.

From the film record, the vertical height of the trace is measured and converted to force F (in pounds). The phase angle, $\emptyset$, between the force and displacement is determined by comparing the vertical distance between the y-intercepts of the trace to the maximum vertical height of the trace (Fig. 11). The dynamic modulus of the elastomer at a particular frequency can be determined by the formula:

$$G = \frac{F/A}{\delta/T}$$

Where F = Measured force amplitude, lbs.
A = Total shear area, $in.^2$
T = Pad thickness, in.
δ = Measured displacement amplitude, in.

For the dimensions of the specimen, the above equation reduces to:

$$G = 0.124 \frac{F}{\delta}$$

The dynamic modulus as a function of frequency is represented in Figs 12 and 13.

Shock Response

To investigate the shock response characteristic of an elastomer and to verify the prediction of the analog computer, a shock in the form of a velocity step is imposed on the elastomer shear pad. It is desirable to introduce a velocity step that produces a stress level within the elastomer of the same order of magnitude as for the frequency response tests. In addition, the mass that is used for the test should be of proper size to allow the natural frequency of the system to be in the mid-range (10 cps) of the previous investigation. Accordingly a 100 lb mass is used.

The most convenient method to introduce a shock is by a swinging pendulum. The length of the pendulum should be long enough so that its natural frequency is much less than the natural frequency of the mass-shear pad combination An overhead height above the shear pad of approximately seven feet is available This permits the length of the pendulum, R, to be 78 in., giving a natural frequency well below that for the mass-shear pad combination.

To insure that the same stress level will occur within the elastomer as in the frequency response investigation, the shear strains imposed on the elastomer for the shock response tests should be the same. An impact velocity of 2 78 in/sec for the 100 lb mass will provide the required shear strain. If the pendulum is displaced horizontally by 1.25 in. and released from rest it will have the required impact velocity.

The signals from the force and displacement transducers are amplified by a Heiland amplifier and then recorded by a Heiland Visicorder. The filter networks used for the frequency response investigation are removed. For a shock response test, two

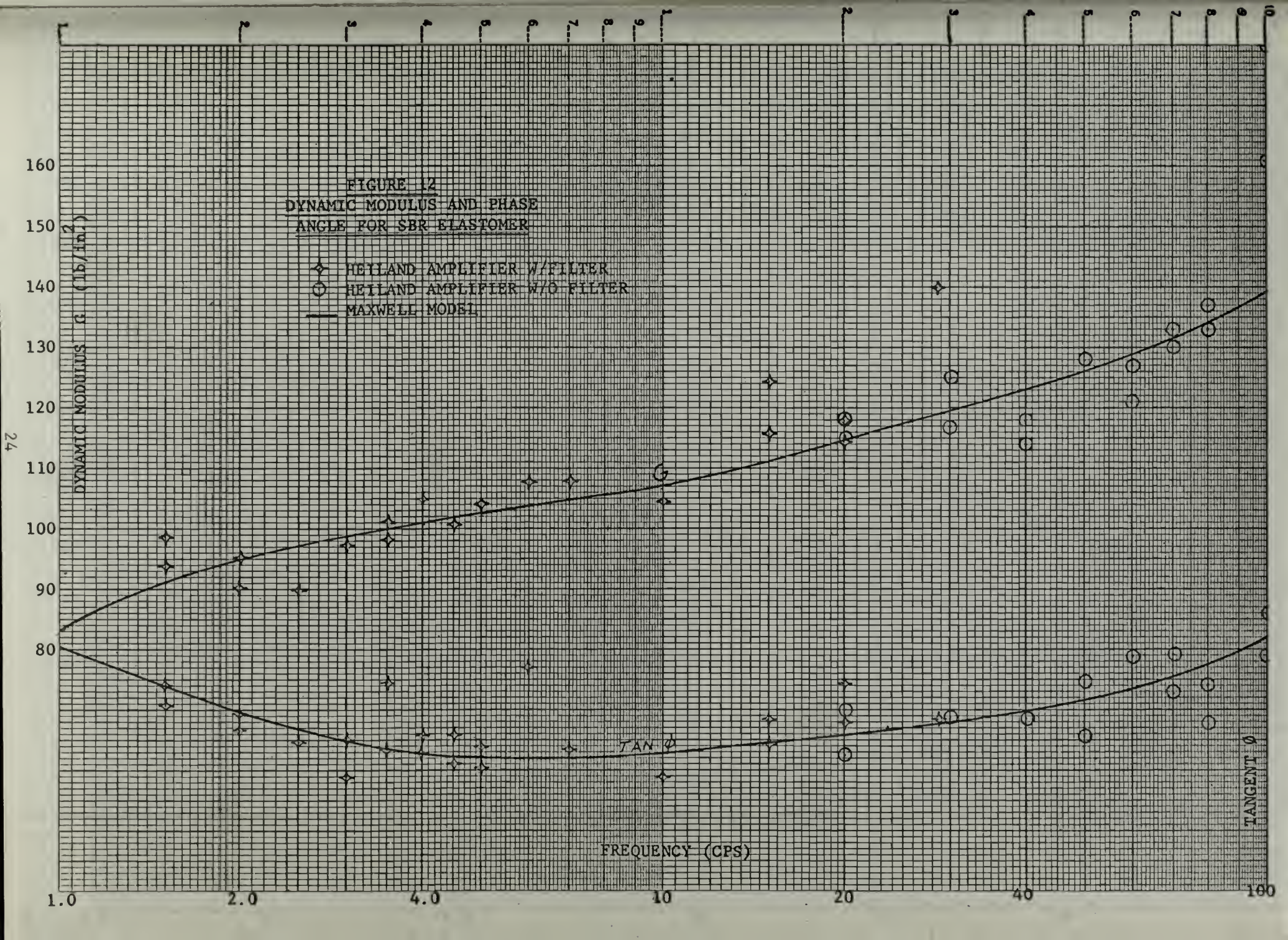
FIGURE 12
DYNAMIC MODULUS AND PHASE ANGLE FOR SBR ELASTOMER
HEILAND AMPLIFIER W/FILTER
HEILAND AMPLIFIER W/O FILTER
MAXWELL MODEL
DYNAMIC MODULUS G (lb/in.²)
TANGENT Ø
TAN Ø
FREQUENCY (CPS)
160
150
140
130
120
110
100
90
80
1.0
2.0
4.0
10
20
40
100

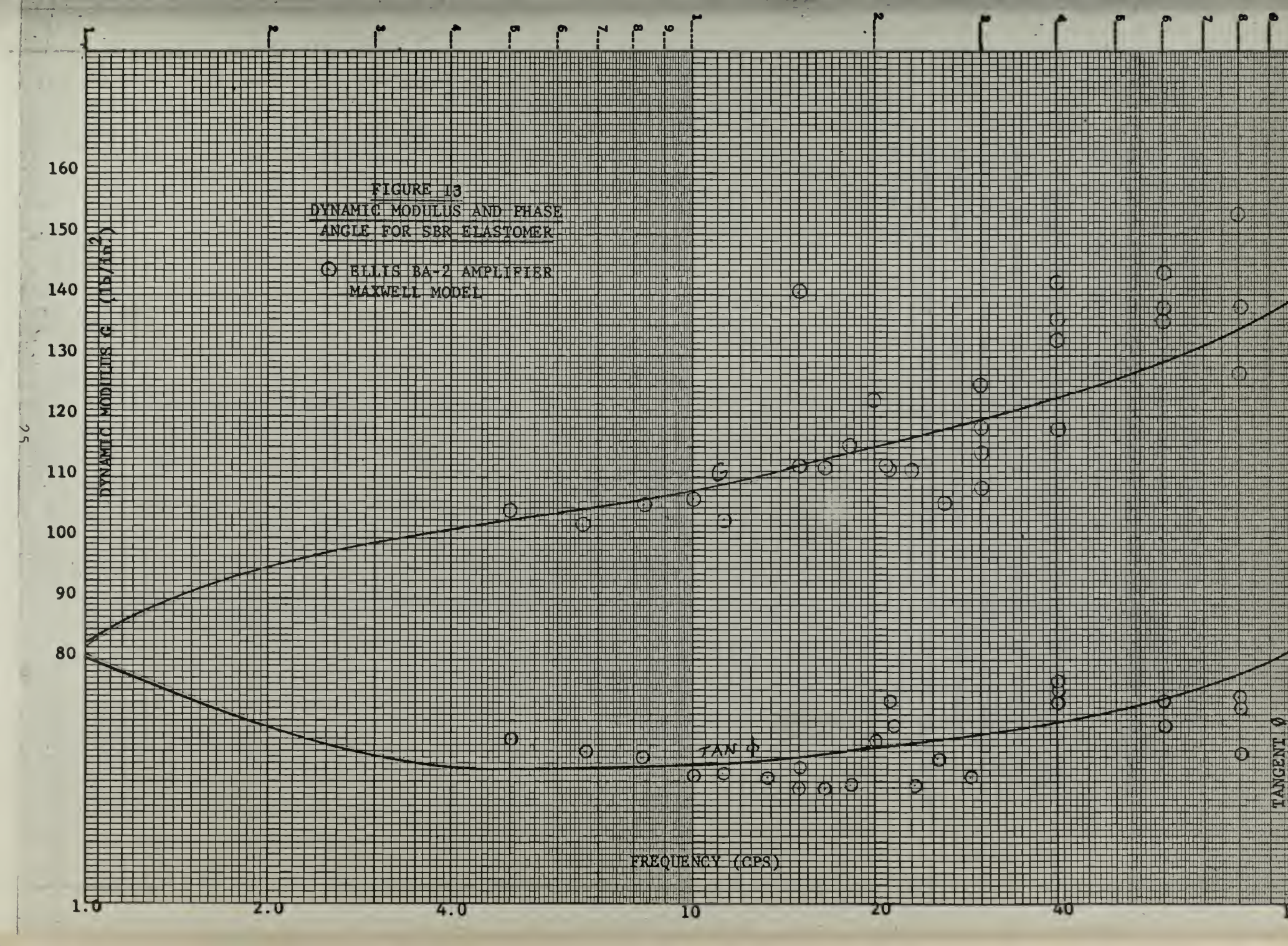
FIGURE 13
DYNAMIC MODULUS AND PHASE ANGLE FOR SBR ELASTOMER
ELLIS BA-2 AMPLIFIER
MAXWELL MODEL
DYNAMIC MODULUS G (LB/IN²)
160
150
140
130
120
110
100
90
80
TAN φ
TANGENT φ
FREQUENCY (CPS)
1.0
2.0
4.0
10
20
40

deflected traces on the recorder tape result ; one for the applied force, and the other for the resulting deflection. In addition to these traces, a time trace is automatically recorded. The interval between the time pulses is 0.01 seconds.

With the pad assembly in its normal horizontal position and after the mass is released just prior to impact, the recording tape is allowed to pay out at a rate of 25 in/sec. Immediately after impact, the tape drive is turned off. A shock record showing force and displacement as a function of time is reproduced in Fig. 14.

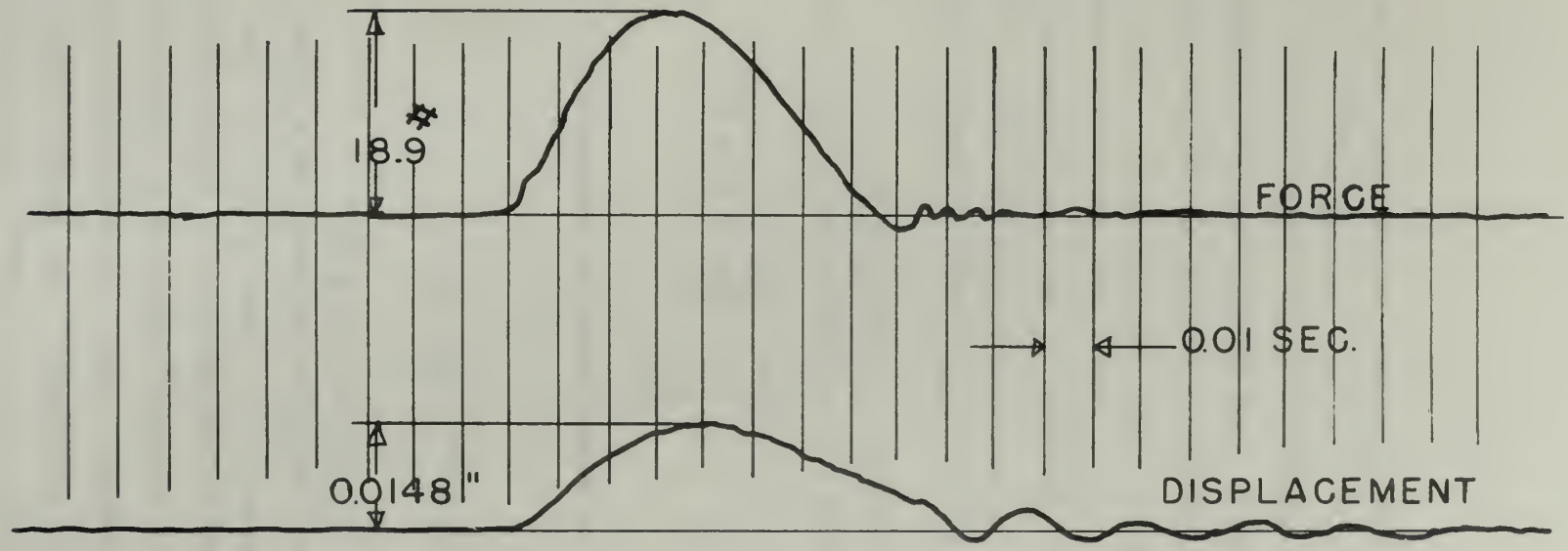

Fig. 14. Shock Response of SBR Elastomer

Chapter IV

SIMULATION OF MODELS BY ANALOG COMPUTERS

Once the dynamic modulus data are reduced, the investigation of the mechanical analog is considered. The dynamic modulus is known as a function of frequency. Also, the phase angle between the applied strain and the resulting stress is a known function of frequency. By equating the spring force to the force developed by the dashpot for each Maxwell unit (Figs. 6 or A-1), the governing equation for each amplifier representing a Maxwell unit in the electronic analog circuit has the form:

$$\dot{\xi}_i + \frac{1}{\tau_i}\,\xi_i = \frac{1}{\tau_i}\,\gamma \qquad 4.1$$

where i = 1, 2, ···,5

The resulting stress in the Maxwell model is represented by the summer amplifier:

$$\frac{\sigma}{G_o} = \gamma + \sum_{i=1}^{i=5} \frac{G_i}{G_o}\left(\gamma - \xi_i\right) \qquad 4.2$$

The schematic wiring diagram for the simulation of the above equations on the analog computer is shown in Fig. 15.

Making an arbitrary choice of the number of Maxwell units, one may attempt to duplicate experimental dynamic modulus results. This requires cut-and-try adjustment of the model parameters τ_i and G_i/G_o. Experience indicates that a more systematic approach is needed for the large frequency range considered here. For this purpose, a frequency distribution of Maxwell units, one decade apart is arbitrarily selected. One Maxwell unit has a dashpot with infinite viscosity. This Maxwell unit has degenerated to a spring. Three Maxwell units have time constants corresponding to a frequency at the bottom (1 cps), middle (10 cps), and top (100 cps) of the range.

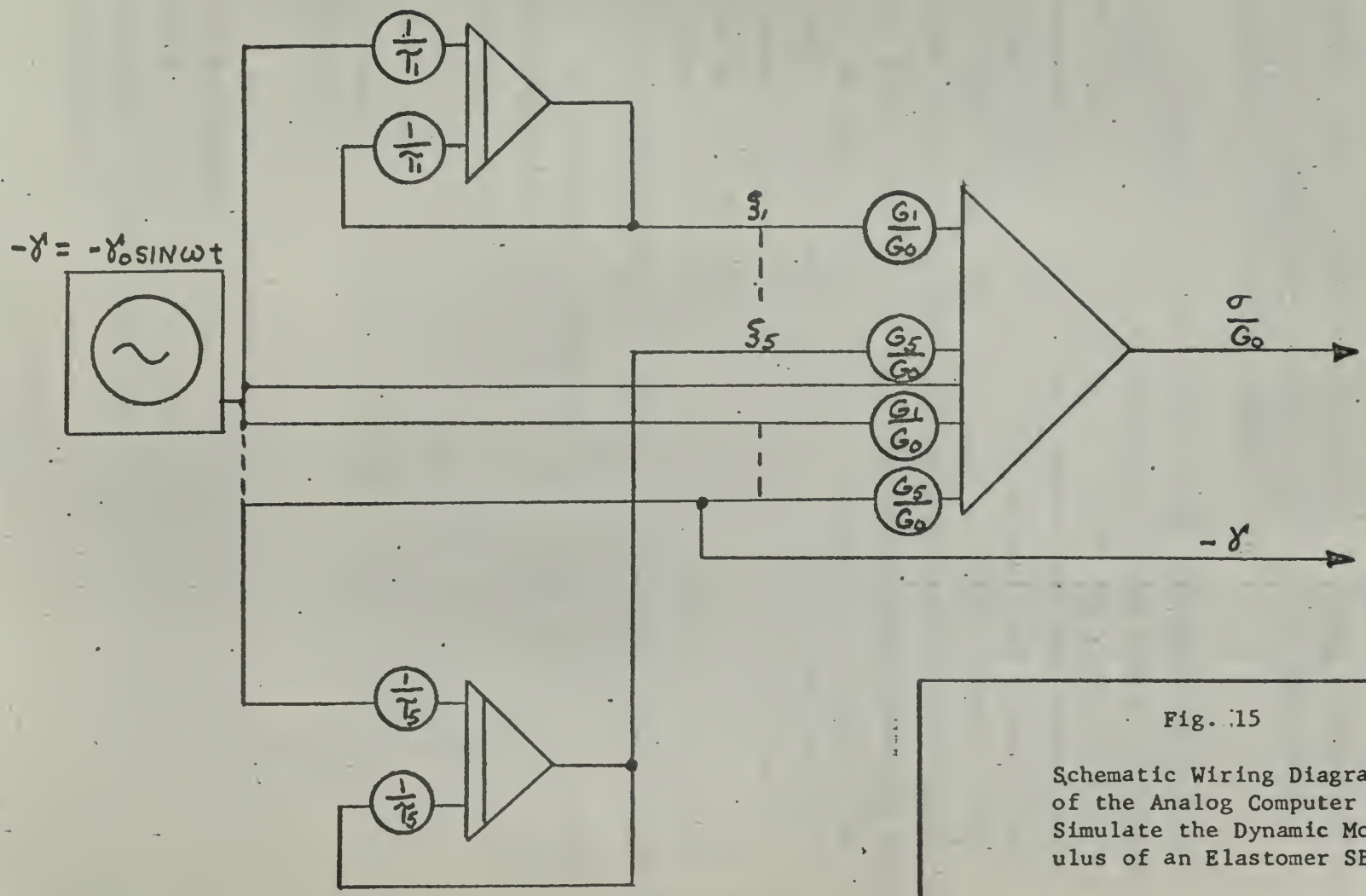

Fig. 15

Schematic Wiring Diagram of the Analog Computer to Simulate the Dynamic Modulus of an Elastomer SBR

Two other Maxwell units are added (one decade below and one decade above the investigation frequency range). Thus, five Maxwell units in parallel with a sixth, a spring, are used to represent the dynamic modulus and phase angle of the SBR elastomer over a two decade frequency range.

To select the proper values of the experimentally derived values of the in-phase and quadrature dynamic modulus components that are to be substituted for G' and G", the accuracy of these data points must first be investigated. The magnitudes of the dynamic modulus when using the Heiland amplifier system without the filter circuit (Fig. 12) appear to be more consistent than those data obtained when using the Ellis BA-2 amplifier system with the filter circuit (Fig. 13). The greater inconsistency of data for the Ellis amplifier system is believed to be caused by the added correction factor required to account for the attenuation characteristics of the filter circuit. Since the results of Heiland based data have fewer correction factors applied, it is assumed that these data more adequately represent the magnitude of the dynamic modulus for SBR over the frequency range 1 to 100 cps.

To obtain the components of the dynamic modulus, the phase angle measurements are required. The spread in these data points appears too large when based on the angle itself. However, the absolute deviations of the magnitude of the quadrature modulus are no greater than those of the dynamic modulus data. A further discussion of the accuracy of the investigation is presented in Appendix C.

By numerical methods, the spring constants G_o through G_5 are determined. From Eqs. A-15 and A-16 the coefficients are first evaluated at the frequencies of 1, 10, and 100 cps. Retaining only coefficients larger than 0.01, the resulting equations are:

$$
\begin{aligned}
0.1\,G_1 + 0.5\,G_2 + 0.1\,G_3 &= 15 \\
G_o + G_1 + 0.5\,G_2 &= 82 \\
0.1\,G_2 + 0.5\,G_3 + 0.1\,G_4 &= 10 \\
G_o + G_1 + G_2 + 0.5\,G_3 &= 103 \\
0.1\,G_3 + 0.5\,G_4 + 0.1\,G_5 &= 21 \\
G_o + G_1 + G_2 + G_3 + 0.5\,G_4 &= 138
\end{aligned}
\qquad 4.3
$$

From these six equations, the six unknowns are determined to have the values:

$G_o = 43$ lb/in.^{2}; $G_1 = 26$ lb/in.^{2}; $G_2 = 25$ lb/in.^{2};

$G_3 = 19$ lb/in.^{2}; $G_4 = 43$ lb/in.^{2}; $G_5 = 9$ lb/in.^{2}

When these values are used to set the potentiometers of the analog circuit, the dynamic modulus and phase angle can be determined as a function of frequency.

To produce a direct comparison to the experimental data, the output signal of the summer amplifier is applied to the vertical plates and the output signal of the sine wave generator is applied to the horizontal plates of an oscilloscope. The resultant trace on the screen will be a Lissajous figure in the form of an ellipse. The procedure to evaluate the dynamic modulus from these ellipses parallels that described for experimental data. Substitution in Eqs. A-15, 16, 17, however, also produces the same results and is a little more direct. The analog curves are compared to the original data in Figs. 12 and 13. Also, the in-phase and quadrature components of the dynamic modulus are presented in Fig. 16.

The final test of the adequacy of the derived mechanical model is provided by comparison with drop test results. Consider

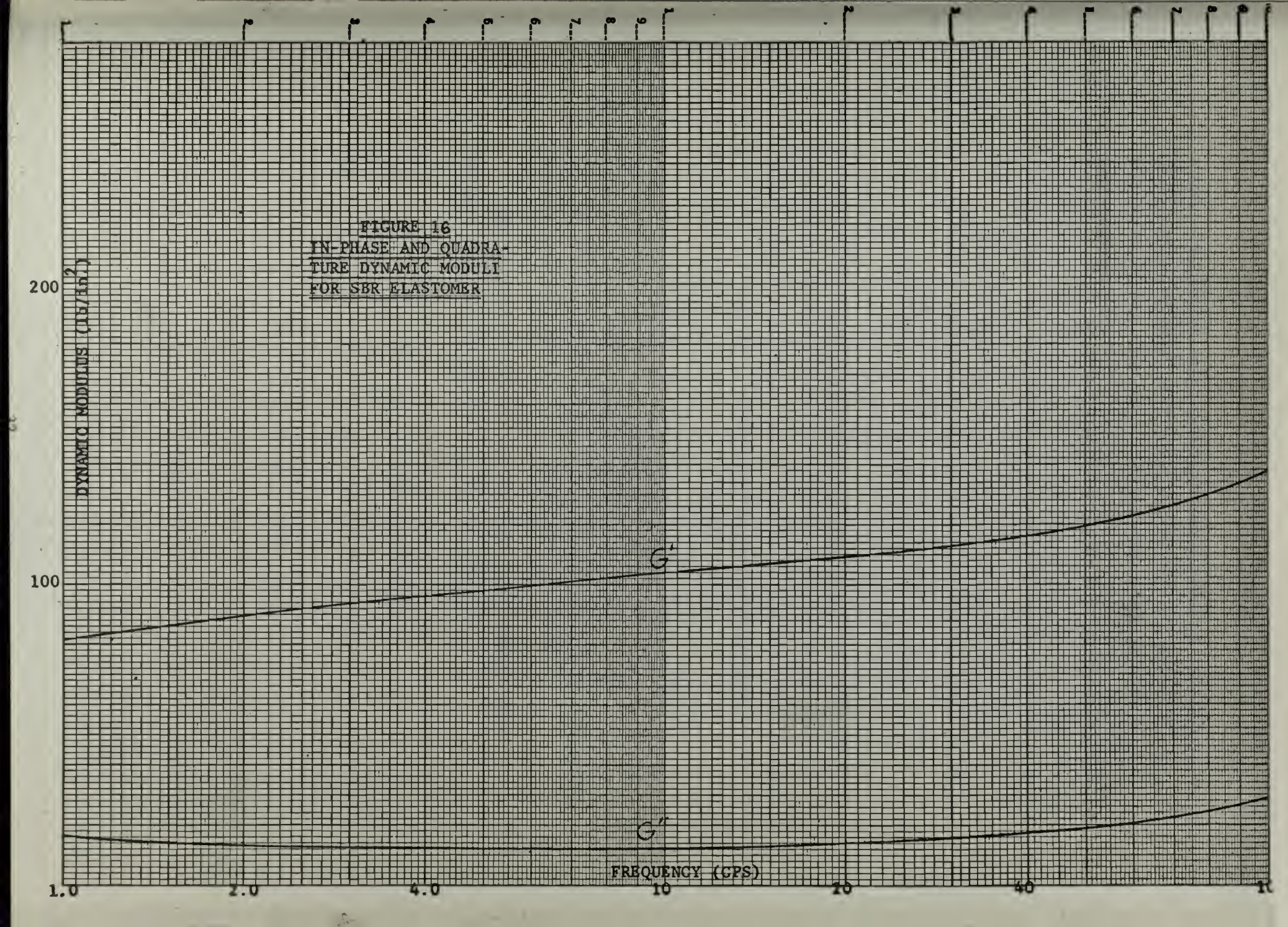
FIGURE 16
IN-PHASE AND QUADRATURE DYNAMIC MODULI FOR SBR ELASTOMER
DYNAMIC MODULUS (lb/in²)
200
100
G'
G''
FREQUENCY (CPS)
1.0
2.0
4.0
10
20
40

a mass M supported by an elastomer shear pad (Fig. 17) having a total cross sectional area A and a thickness T. Defining $x = w - u$ and $y_i = w - v_i$, the equation of motion can be expressed as:

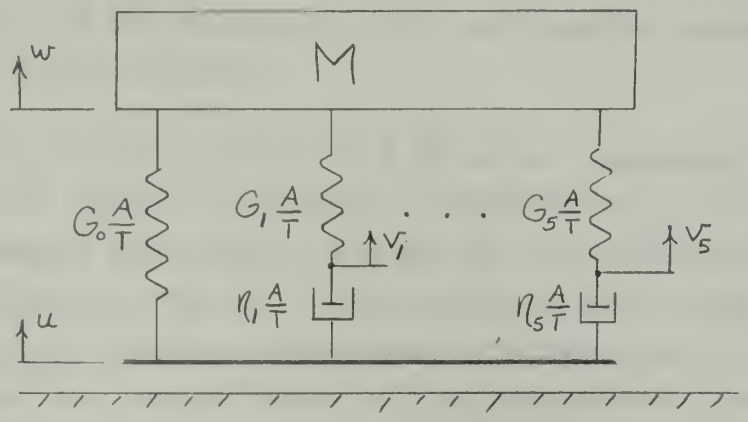

Fig. 17 Model for Simulating Shock Test

$$\frac{\ddot{x}+\ddot{u}}{\omega_o^2} + X + \sum_{i=1}^{i=5} \frac{G_i}{G_o} Y_i = 0 \qquad 4.4$$

where $\omega_o^2 = \frac{G_o A}{M T}$

For the shock response test, it is assumed that the acceleration $\ddot{u}$ is zero and the velocity $\dot{u}$ at impact is 2.78 in./sec.

The equality of forces in the spring and dashpot of a Maxwell unit can be represented by the equation:

$$\eta_i(\dot{u} - \dot{v}_i) = G_i(w - v_i)$$

or

$$\dot{Y}_i = -\left(\dot{x} - \frac{1}{\tau_i} Y_i\right) \qquad 4.5$$

where i = 1, 2, ..., 5

The analog computer simplifies prediction of the corresponding model behavior. The circuit diagram is shown in Fig. 18. Equation 4.4 is represented by the summer amplifier. Five integrating amplifiers represent Eqs. 4.5. The analog solution to the above equations applies only to the first half-cycle of motion of the striking pendulum; for the second half-cycle the pendulum separates from the shear pad striker plate.

For an impact velocity of 2.78 in/sec, equivalent to a momentum at impact of one lb-sec, a maximum force of 19 lbs and a maximum displacement of 0.015 in. are predicted by the analog computer (Fig. 19). The averages of four shock response runs indicate that the maximum force and displacement are 18.3 lbs and 0.0162 in , respectively; or a 4% difference in force and an 8% difference in displacement measurements. Indeed, the technique to predict the dynamic response characteristics of an elastomer, described above, does provide adequate results.

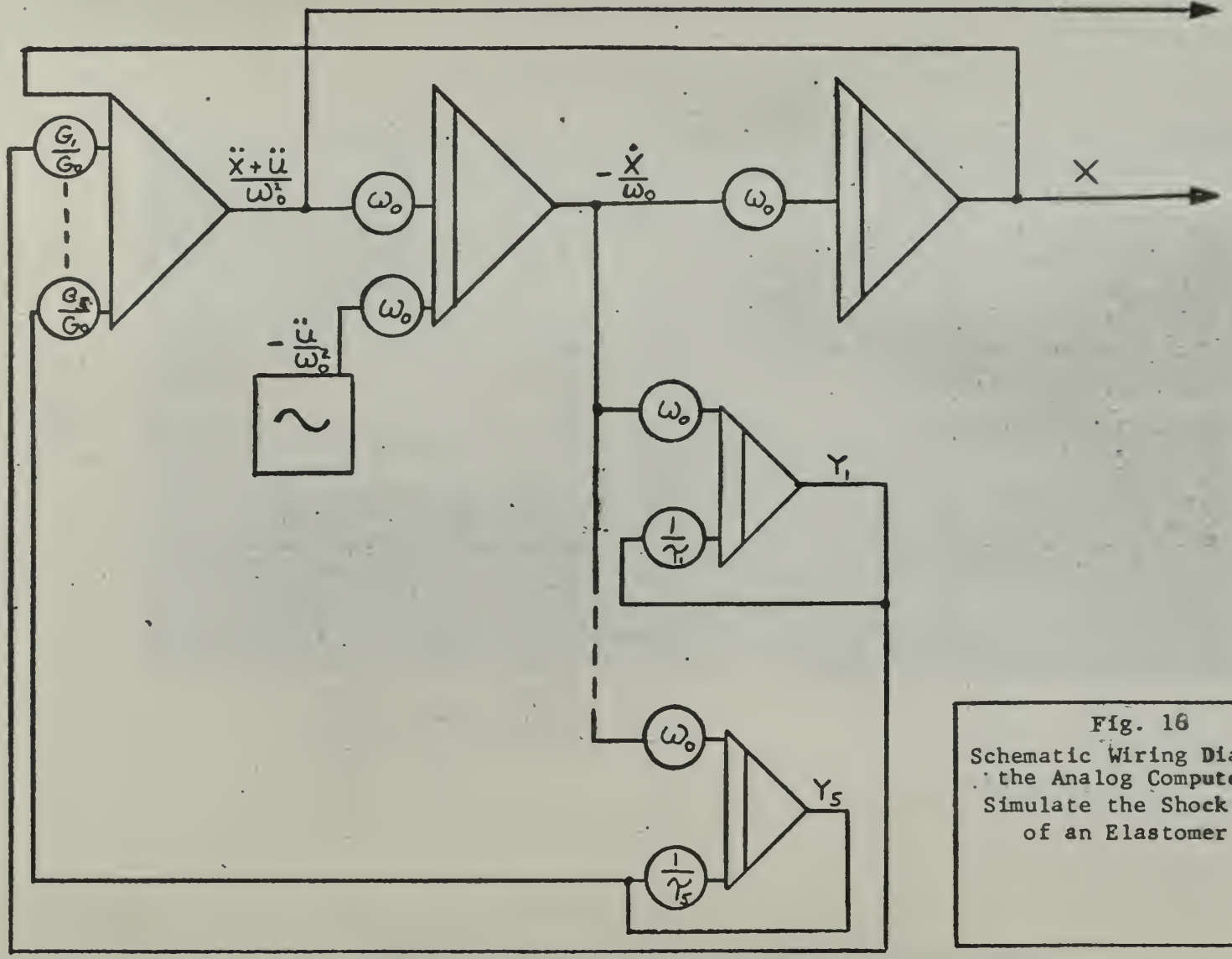

Fig. 16
Schematic Wiring Diagram of the Analog Computer to Simulate the Shock Response of an Elastomer SBR

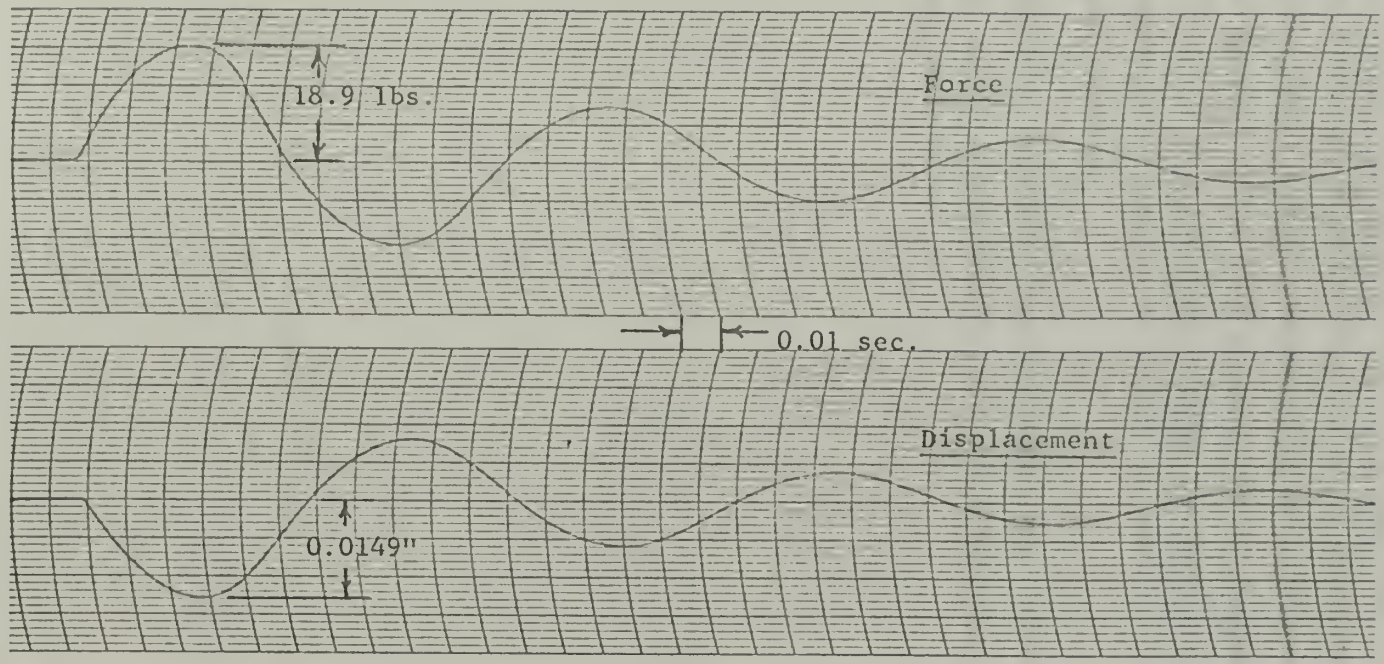

Fig. 17. Analog Solution of Shock Response of SBR

Chapter V

CONCLUSIONS AND RECOMMENDATIONS

The Maxwell representation, in conjunction with the use of an analog computer, appears to provide an adequate method to predict the linear dynamic behavior of an elastomer. The arbitrary choice of Maxwell units with characteristic frequencies spaced at decade intervals and spanning a range two decades larger than the range investigated appears to permit an adequate representation of the dynamic modulus.

Since this technique was developed and tested for only one elastomer, it is recommended that other elastomers be tested to verify this procedure.

BIBLIOGRAPHY

1. A. T. McPherson and A. Klemin, ENGINEERING USES OF RUBBER, Reinhold, (1956).

2. W. Voigt, Ann. Physik, 47,671, (1892).

3. R. E. Newton and L. E. Matthews, SAE Preprint No. 236B, (1960).

4. J. C. Maxwell, Phil. Trans. Roy. Soc. 157,49 (1867).

5. T. Alfrey, MECHANICAL PROPERTIES OF HIGH POLYMERS, Interscience, New York, (1948).

6. B. Gross, MATHEMATICAL STRUCTURE OF THE THEORIES OF VISCO-ELASTICITY, Hermann, Paris, (1953).

7. W. Kuhn, Z. Physik Chem. B42, (1939).

8. R. F. Tuckett, Trans. Faraday Soc., 38 310, (1942).

9. R. S. Stein and A. V. Tobolsky, J. Poly. Sci., 7, 221, (1957).

10. R. J. Roark, FORMULAS FOR STRESS AND STRAIN, D. Van Nostrand, (1958).

11. R. B. Blizard, J. Appl. Phys. 22, 730, (1951).

12. J. H. Dillon and S. D. Gehman, India Rubber World, 115, 61-8, 76, 217-22, (1946).

13. J. D. Ferry, J. Appl. Phys. 24, 911, (1953).

14. A. V. Tobolsky and G. M. Brown, J. Polymer Sci., 17, 547, (1955).

15. M. Samec, ELASTOMERS AND PLASTOMERS, Elsevier's Polymer Series 1, 241, (1950).

16. F. B. Hildebrand, ADVANCED CALCULUS FOR ENGINEERS, 444, (1949).

17. J. E. Ruzicka, "Forced Vibration in Systems with Elastically Supported Damper", MS Thesis, MIT, (1957).

18. H. Leaderman, RHEOLOGY, 2, 137, (1958).

19. J. A. Van Den Broek, ELASTIC ENERGY THEORY, Wiley, (1953).

20. J. P. Den Hartog, MECHANICAL VIBRATIONS, McGraw Hill, (1947).

21. C. C. Perry and H. R. Lissner, THE STRAIN GAGE PRIMER, McGraw Hill, (1955).

22. H. Chestnut and R. W. Mayer, SERVOMECHANISMS AND REGULATING SYSTEM DESIGN, Wiley, (1951).

23. H. Diederichs and W. C. Andrae, EXPERIMENTAL MECHANICAL ENGINEERING, Wiley, (1930).

APPENDIX A

APPLICABLE FORMULAE FOR THE MAXWELL MODEL

The mechanical model analyzed in this appendix is the Maxwell model representation for a cross-linked elastomer. The model orientation and the assumed system constants appear in Fig. A-1. Conventional methods are used to solve for the dynamic modulus as a function of frequency.

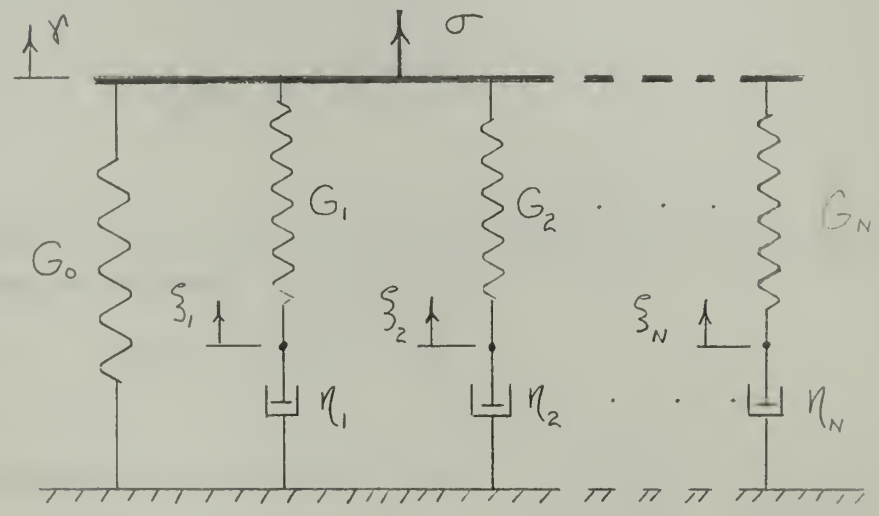

Fig. A-1

Consider the Maxwell model of Fig. A-1. We may define γ_i to be the stretch of the spring in the i th Maxwell unit so that

$$\gamma_i = \gamma - \xi_i \qquad \text{A-1}$$

$$i = 1, 2, \ldots, N$$

Summing the spring forces gives

$$\sigma = G_0 \gamma + \sum_{i=1}^{i=N} G_i \gamma_i \qquad \text{A-2}$$

For each Maxwell unit:

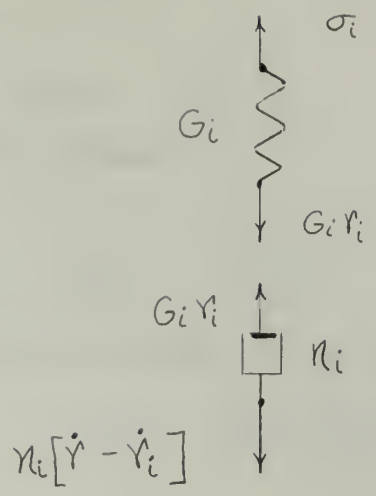

Fig. A-2

where the ($\dot{}$) indicates the derivative with respect to time. The following relationship is obtained:

$$G_i\gamma_i = \eta_i\left[\dot{\gamma} - \dot{\gamma}_i\right]$$

$$i = 1, 2, \ldots, N \qquad \text{A-3}$$

or, in terms of the relaxation time $\tau_i = \frac{\eta_i}{G_i}$ Eq. A-3

can be rewritten in the form:

$$\dot{\gamma}_i + \frac{1}{\tau_i}\gamma_i = \dot{\gamma} \qquad \text{A-4}$$

$$i = 1, 2, \ldots, N$$

Letting

$$\gamma = \gamma_o \sin \omega t \qquad \text{A-5}$$

and

$$\gamma_i = A_i \sin \omega t + B_i \cos \omega t \qquad \text{A-6}$$

and substituting into Eq. A-4

$$\omega A_i \cos \omega t - \omega B_i \sin \omega t + \frac{1}{\tau_i}\left(A_i \sin \omega t + B_i \cos \omega t\right) = \omega \gamma_o \cos \omega t \qquad \text{A-7}$$

Collecting like terms

$$-\omega B_i + \frac{1}{\tau_i} A_i = 0 \qquad \text{A-8}$$

and

$$\omega A_i + \frac{1}{\tau_i} B_i = \omega \gamma_o' \qquad \text{A-9}$$

Solving Eq. A-8 we obtain:

$$B_i = \frac{A_i}{\tau_i \omega} \qquad \text{A-10}$$

Substituting Eq. A-10 into Eq. A-9 we thus obtain:

$$A_i = \gamma_o \frac{(\tau_i \omega)^2}{1 + (\tau_i \omega)^2} \qquad \text{A-11}$$

and

$$B_i = \gamma_o \frac{(\tau_i \omega)}{1 + (\tau_i \omega)^2} \qquad \text{A-12}$$

Therefore

$$\gamma_i = \gamma_o \frac{(\tau_i \omega)^2}{1 + (\tau_i \omega)^2} \sin \omega t + \gamma_o \frac{(\tau_i \omega)}{1 + (\tau_i \omega)^2} \cos \omega t \qquad \text{A-13}$$

Substituting Eqs. A-13 and A-5 into Eq. A-2 and dividing by the shearing strain amplitude γ_o, we obtain.

$$\frac{\sigma}{\gamma_o} = \left\{ G_o + \sum_{i=1}^{i=N} G_i \frac{(\tau_i \omega)^2}{1 + (\tau_i \omega)^2} \right\} \sin \omega t + \left\{ \sum_{i=1}^{i=N} G_i \frac{(\tau_i \omega)}{1 + (\tau_i \omega)^2} \right\} \cos \omega t \qquad \text{A-14}$$

The component of the modulus that is in-phase with the applied shearing strain is called the storage modulus or in-phase dynamic modulus, G':

$$G' = G_o + \sum_{i=1}^{i=N} G_i \frac{(\tau_i \omega)^2}{1 + (\tau_i \omega)^2} \qquad \text{A-15}$$

The component that is 90^{o} advanced in phase from the applied strain is called the loss modulus or quadrature dynamic modulus, G":

$$G'' = \sum_{i=1}^{i=N} G_i \frac{(\tau_i \omega)}{1 + (\tau_i \omega)^2} \qquad \text{A-16}$$

The properties of an elastomer are specified either by G' and G" or by the dynamic modulus G and a phase angle ϕ . The dynamic modulus is simply the absolute value of the complex modulus and is given by the equation:

$$G = |G^*| = \left\{ [G']^2 + [G'']^2 \right\}^{1/2} \qquad \text{A-17}$$

The associated phase angle measured from the applied strain is given by:

$$\phi = \tan^{-1} \frac{G''}{G'} \qquad \text{A-18}$$

APPENDIX B

DETAIL DESIGN OF EXPERIMENTAL EQUIPMENT

Transducer Properties

The force transducer as described in Chapter III is a two inch diameter steel ring with a cross section of 0.098" x 1 0" (Fig. B-1) Mounted diametrically opposite and perpendicular to the load axis are four Bakelite flats. Bonded to each flat is an SR-4, 2000 ohm, Type C-14 strain gage A ring transducer was selected on the basis that this geometry provides a good combination of structural stiffness and relatively high stresses

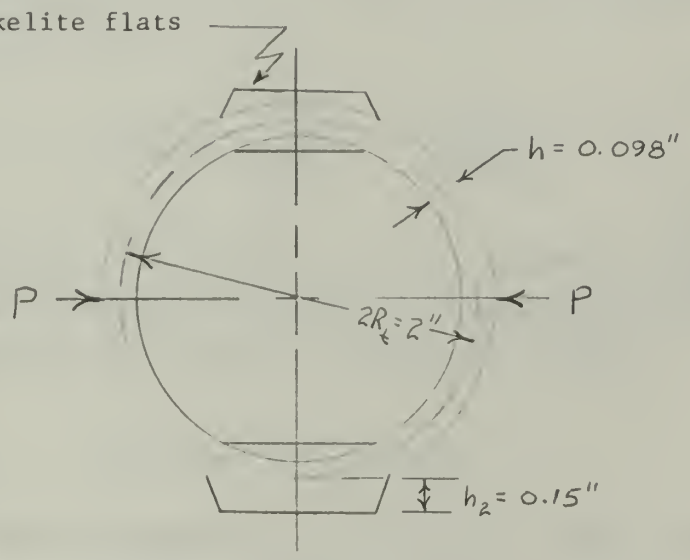

Fig. B-1 Force Transducer

For an applied load P (Fig. B-1) the stress at the surface of the steel ring is given by the equation:

$$\sigma_b = \frac{M\ h/2}{I} \qquad \text{B-1}$$

where $M = -0.1817\ PR_t$ Ref. 10

The corresponding strain a strain gage would experience at this point of the steel ring is:

$$\epsilon = \frac{\sigma_b}{E} = 3.6\,P \ \mu\text{in./in.} \qquad \text{B-2}$$

To increase the magnitude of this strain value Bakelite flats are provided. The Bakelite flats provide an increase in the distance from the neutral axis. If the stiffening effects of the Bakelite flats are neglected, the strain becomes:

$$\epsilon = 10.9\,P \ \mu\text{in./in.}$$

The spring constant K_t for a ring of uniform cross-section is given by the equation:

$$K_t = \frac{P}{2\delta_r} = \frac{EI}{0.137\,R_t^3} \qquad \text{B-3}$$

Ref. 19

and has a value K_t = 18,210 lb/in. If the stiffening effect of the Bakelite flats is taken into account, an analysis by standard methods[19] gives for the strain as a function of load:

$$\epsilon = 8.85P\ \mu\text{in/in.}$$

The spring constant becomes K_t = 21,610 lb/in. Since the force transducer has a spring constant approximately 27 times that of the rubber sample, the transducer deflections are neglected By hanging a known weight from the transducer and recording the strain with an SR-4, Type N, strain indicator, the actual strain as a function of load was determined as $\epsilon = 6.04\,P\ \mu\text{in./in.}$

Since four strain gages are used, the strain as a function of load for the force transducer is: $\epsilon = 24.16\ \mu\text{in./in./lb}$

At higher frequencies it is important to recognize that the force indication of the transducer includes the inertia forces on the connector plate and a portion of the ring The system may be idealized as shown below (Fig B-2). The left-hand spring (stiffness K_t) represents the elasticity of the transducer, the mass m represents the connector plate together with a certain effective mass contributed by the transducer, and the right hand spring represents the elasticity of the rubber (complex stiffness Z).

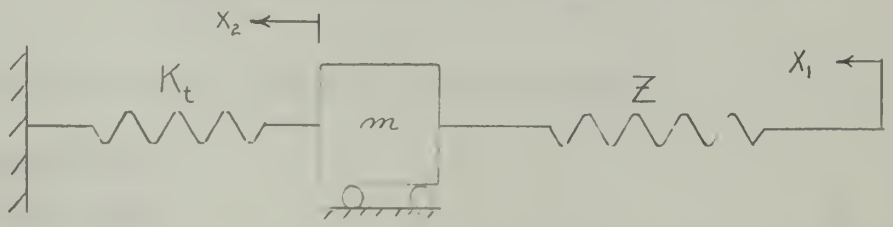

Fig. B-2

The equation of motion of the mass is:

$$m\ddot{X}_2 - Z(X_1 - X_2) + K_t X_2 = 0 \qquad \text{B-4}$$

or

$$\ddot{X}_2 + \left(\frac{Z}{K_t} + 1\right)\omega_t^2 X_2 = \frac{Z}{K_t}\omega_t^2 X_1 \qquad \text{B-5}$$

where $\omega_t^2 = K_t/m$

If $x_1 = a_1 e^{j\omega t}$ and $x_2 = a_2 e^{j\omega t}$, the force amplitude transmitted by the transducer is:

$$P = K_t a_2 = \frac{Z a_1}{\left(\frac{Z}{K_t} + 1\right) - \frac{\omega^2}{\omega_t^2}} \qquad \text{B-6}$$

If $K_t >> R_e(Z)$ then

$$P = \frac{Z a_1}{1 - \frac{\omega^2}{\omega_t^2}} \qquad \text{B-7}$$

The measured frequency of the ring with masses attached is 129 cps. It is noted that the effect of the added mass is to increase the indicated force reading as the forcing frequency approaches the natural frequency of the ring. For data reduction, it is assumed that the force Za_1 in the specimen is related to the indicated force P by solving Eq. B-7 to obtain:

$$Za_1 = P\left[1 - \frac{\omega^2}{\omega_t^2}\right] \qquad \text{B-8}$$

The frequency ω_t is taken to be 810 rad/sec.

Instrumentation

Strain Gages

The strain gage is used to convert strain to an electrical output. This output should be high as possible to minimize the necessary amplifier gain. Since the measurements are dynamic, a dynamic type gage is advantageous

The 2000 ohm SR-4, Type C-14, strain gage with a gage factor of 3.11 has the maximum output of all dynamic gages. W. T. Bean[21] recommends a maximum strain gage sensitivity, ΔE, of 160 millivolts per active gage and is based on 50 milliamperes current per gage and 1000 micro-inches per in. of strain. The Bakelite flats limited the amount of heat dissipated and the bridge voltage had to be reduced from 100 volts to 28 volts. On this basis, the calculated load sensitivity is $\Delta E/P = 0.52$ millivolts/lb. Therefore, some amplification of the signal is required.

For the displacement transducer, the required output sensitivity is easily obtained. For the purpose, 500 ohm SR-4 gages, Type C-7, are mounted near the root of a cantilever beam (.032" x½" x2.5").

Amplifiers and Filter Circuits

As stated in the previous section, amplification of the output signal of the force transducer is required. As soon as amplification

of the signal is provided, some unwanted noise is amplified as well. To reduce the noise and have a clear trace on the oscilloscope a low pass filter circuit is provided. The electrical circuit diagram for the instrumentation appears in Fig. 9.

The signal from the force transducer, when filtered, is attenuated. The degree of attenuation is a function of frequency For the circuit in Fig. B-3 the circuit parameters are:

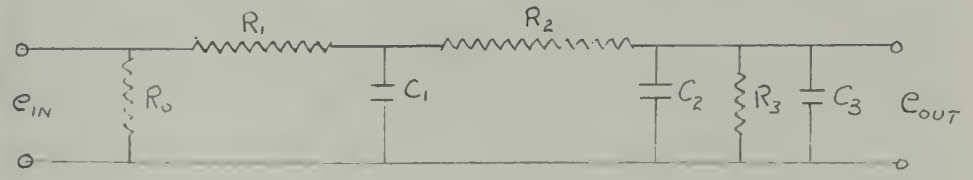

Fig. B-3 Filter Circuit

where R_1 = 0.73 Megohm

C_1 = 0.0065 μf

R_2 = 0.675 Megohms

C_2 = 0.0068 μf

Oscilloscope input impedance

R_3 = 2.0 Megohm

C_3 = 25 $\mu\mu f$

Amplifier output impedance (BA-2)

R_o = 2 Megohm

The attenuation ratio e_{out}/e_{in} as a function of frequency is found by standard methods[22].

The resultant attenuation curves appear in Fig. B-4. Curve 1 is the attenuation of the filter alone as a function of frequency. This is used with the Heiland amplifier. Curve 2 is the attenuation accounting for an amplifier output impedance of 2 megohm. This is used with the Ellis BA-2 amplifier.

Calibration

With the connector plate and specimen removed, a calibrated leaf spring is connected between the transducer and the specimen

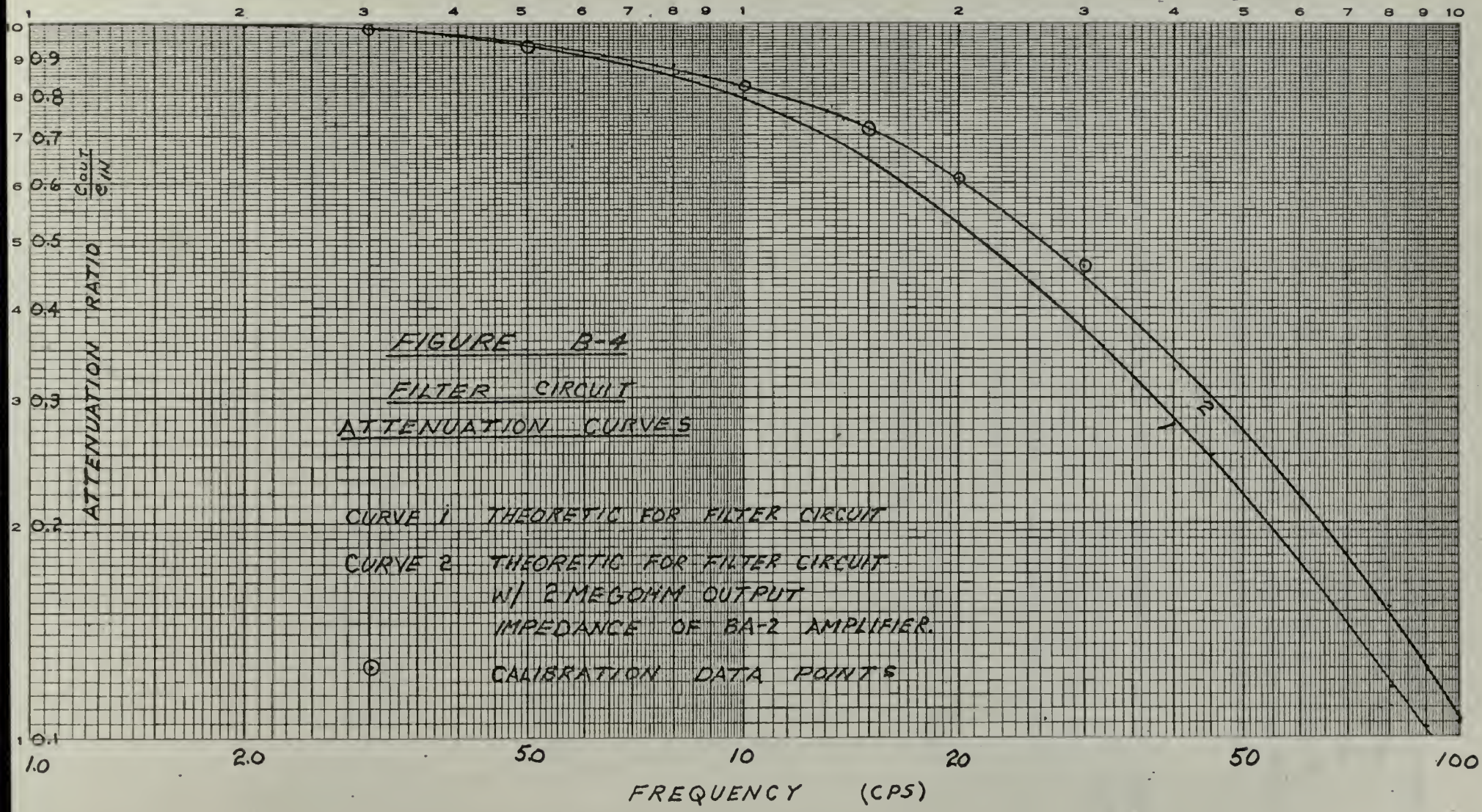
ATTENUATION RATIO $\frac{E_{OUT}}{E_{IN}}$
FREQUENCY (CPS)
1.0
2.0
5.0
10
20
50
100
0.1
0.2
0.3
0.4
0.5
0.6
0.7
0.8
0.9
1
2
3
4
5
6
7
8
9
10
FIGURE B-4
FILTER CIRCUIT
ATTENUATION CURVES
CURVE 1 THEORETIC FOR FILTER CIRCUIT
CURVE 2 THEORETIC FOR FILTER CIRCUIT W/ 2 MEGOHM OUTPUT IMPEDANCE OF BA-2 AMPLIFIER.
CALIBRATION DATA POINTS

holder. If the holder is given a sinusoidal displacement, a known force is being transmitted to the ring transducer. The spring constants k of two steel leaf springs, 1/32" x 1/2" x 5.5" and 0.098" x 1/2" x 5.5", were determined by supporting a weight at the center of the beam and measuring its mid span deflection with a microscope. The two leaf springs have spring constants of 69 lb/in and 1050 lb/in., respectively.

The thinner leaf spring was used to calibrate the force transducer below a force level of 4 pounds Above this value, the 0 098" thick leaf spring was used. Since the calibration of the force transducer was performed under dynamic conditions, the inertia effects of the beam must be considered.

The leaf spring is assumed to act as two cantilever beams whose deflection curve has the form shown.

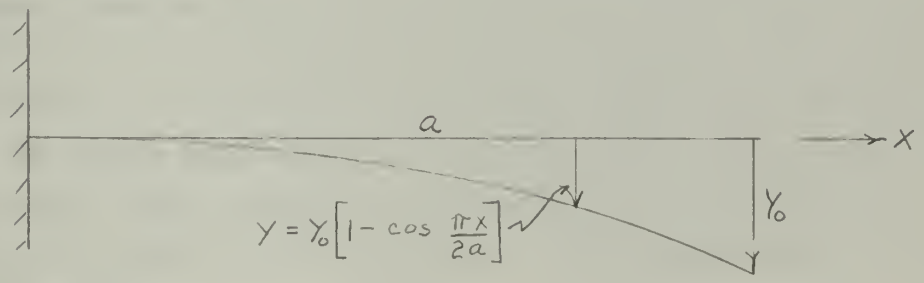

Fig. B-5

It can be shown that the circular natural frequency of a beam having a mass per unit length μ is given by the equation:

$$\omega_B = 3.62\sqrt{\frac{EI}{\mu a^4}} \qquad \text{B-9}$$

For the 1/32 in. thick steel member, the natural frequency $f_b = \omega_B/2\pi$ is 92.4 cps and for the 0.098 in. member, the natural frequency is 290 cps.

The measured force P at the transducer as a result of a sinusoidal displacement $Y_o = \delta_o \sin\omega t$ is given by:

$$P = \frac{6EI}{a^3} Y_o \left[1 + 0.59 \frac{\omega^2}{\omega_B^2} \right] \qquad \text{B-10}$$

or, in terms of the static spring constant k,

$$P = k Y_o \left[1 + 0.59 \frac{\omega^2}{\omega_B^2} \right] \qquad \text{B-11}$$

To insure that the signals from the strain gages of the force transducer have a consistent datum, the calibration chopper signal from the BA-2 amplifier is used. Normally the calibration signal when applied to the vertical plates of the oscilloscope is a square wave whose frequency is approximately 85 cps. With the low pass filter circuit, the resultant trace is a sine wave. For a five megohm resistor shunted across one of the active gages, the double amplitude of the unfiltered square wave measured 48 millivolts. By Fourier series analysis, the double amplitude of the fundamental of the square wave should be 58.5 millivolts. The attenuation of the input signal from Fig. B-4, curve 2, is 0.14 at 85 cps or a resultant signal of 8.2 millivolts. The measured signal is 8.4 millivolts.

It is therefore assumed that all the attenuation is being provided by the filter circuit and the reference calibration of 8.4 millivolts will be used.

If a deviation in the calibration signal does occur due to change in bridge voltage or amplifier gain, the vernier adjustment provision on the oscilloscope can bring the signal to the desired height. Based on the assumption that the output signal ratio will vary linearly for the remaining circuitry of the oscilloscope, it is assumed that this calibration procedure is correct.

Once the calibration datum is assured, the calibration of the force transducer is now possible. A statically calibrated leaf spring is connected between the transducer and the specimen holder. For a particular displacement double amplitude of the eccentric, the resulting signal from the transducer is amplified, filtered, and then applied to the vertical plates of the oscilloscope. The double amplitude of the trace on the oscilloscope screen is then recorded at a particular frequency. With the displacement amplitude at a known value, this procedure is repeated for selected frequencies in the range of 1 to 30 cps. These points are plotted in Fig. B-4.

Not only are the filter characteristics included in the calibration measurements, but the mass effects of the calibration beam and force transducer are measured as well. From Eqs. B-8 and B-11 the mass effects can be determined. The force transducer constant for strain as a function of load (24.16 μ in./in./lb), Eq. B-8 and Fig. B-4 are used as the calibration parameters. For the BA-2 amplifier with two stages of amplification the calibration constant is 8.99 millivolts per pound. The calibration constant for the Heiland system with the gain set at 1.25 is 45.6 millivolts per pound without the filter circuit. When the Heiland amplifier is used with the filter circuit in place, Curve 1, Fig. B-4 is used to correct for the difference in attenuation characteristics.

APPENDIX C

ACCURACY OF EXPERIMENTAL RESULTS

The errors of observation for any experimental investigation can be classified as: accidental, those whose occurrence cannot be foreseen; personal errors, due to the habits of a given person; and instrumental errors, due to improper calibration. The major sources of errors are the latter two These are generally combined in one major grouping called "Systematic Errors".[23] The remaining discussion is directed to this area.

From the initial calibration signal height of 8.4 cm. and the resulting force prediction described in Chapter III for the force transducer, with the filter circuit in place, the calibration of the force transducer is believed to be accurate to within 3% for forcing frequencies below 30 cps. For frequencies above 30 cps, the inertial effects of the ring transducer and the attached masses should be taken into account.

The experimentally derived dynamic modulus data is presented in two forms: one representing data obtained using the Ellis BA-2 amplifier system (Fig. 13) and the other (Fig. 12) using the Heiland system. Based on the assumed Maxwell model characteristics the maximum derivation of a single data point for the first system is approximately 25%; while for the latter, the maximum deviation is 17%. The average absolute value of the deviation of data for the Heiland system is about 8% and is consistent throughout the frequency range. The data points at 100 cps in Fig. 12 are omitted from these comparisons. These values were obtained for small displacements and thus the uncertainties of the actual displacement that the elastomer experiences permits the rejection from consideration of these data points.

The average absolute value of deviation of data points for the Ellis amplifier system is approximately equal to the maximum

deviation for the Heiland system. This larger spread is believed to be caused by the additional correction factor required to account for the attenuation characteristics of the filter circuit used in the force amplifier circuit (Fig. 9). The uncertainty of the exact characteristics of the filter circuit and uncertainty of the effect of the output impedance of the Ellis amplifier may account for this larger spread in data.

The deviation for the phase angle measurements is approximately the same for both cases. This indicates that the procedure to evaluate the phase angle has room for improvement. If the deviation is expressed as a fraction of the dynamic modulus, the deviation of the quadrature component is no greater than that of the dynamic modulus.

The dynamic modulus found is in consonance with values reported in the literature. At a frequency of approximately 3 cps, the dynamic modulus for SBR having a Shore Hardness of 56 at 70^{o}F is given as 100 lb/in^2. [1] The author has a tolerance associated with this value of $\pm$17%. The test data presented give a dynamic modulus of 99 lb/in^2, well within the stated tolerance range. It is believed that the dynamic modulus values represented by the adopted Maxwell model (solid curve of Fig. 12) are accurate within 10% for the sample tested.

The final comparison is that of the predicted shock response of an elastomer. Although excellent results are realized in this prediction, one can only assume that from the processes of determining the frequency response, converting these data to an appropriate Maxwell model, and then the final prediction of the shock response, the expected error of this technique is not greater than 15%.

APPENDIX D

DYNAMIC MODULUS TEST DATA

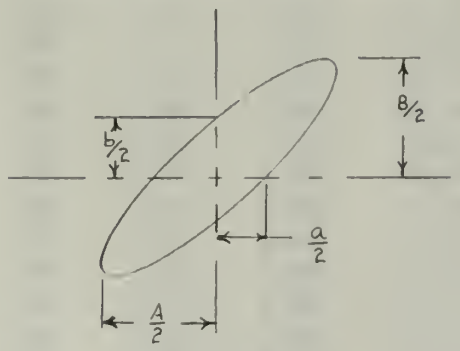

Fig. D-1

f cps	2δ in.	S mv/cm	A cm	B cm	a cm	b cm	Rmks
1.5	0.0270	50	6.30	3.83	1.07	0.64	H
	0.0270	20	6.40	9.20	0.97	1.40	H
2	0.0270	50	6.50	3.74	0.98	0.41	H
	0.0270	50	3.75	3.52	0.52	0.53	H
2.5	0.0270	20	7.10	8.80	0.90	1.06	H
3	0.0270	50	3.80	3.74	0.50	0.47	H
	0.0270	50	5.30	3.75	0.41	0.43	H
3.5	0.0270	50	4.50	3.85	0.54	0.46	H
	0.0270	20	5.10	9.42	0.89	1.56	H
4	0.0270	20	5.40	9.92	0.63	1.26	H
	0.0270	20	5.40	9.92	0.64	1.36	H
	0.0270	50	5.20	3.97	0.62	0.47	H
4.5	0.0270	20	5.00	9.42	0.63	0.84	H
	0.0270	50	5.80	3.80	0.77	0.47	H
5	0.0270	50	6.40	3.83	0.77	0.47	H
	0.0270	50	7.90	3.82	1.10	0.47	E
	0.0270	50	4.80	3.88	0.39	0.49	H
6	0.0270	50	5.10	3.95	0.94	0.48	E
6.6	0.0270	50	7.78	3.84	0.90	0.48	E
7	0.0270	50	6.41	3.32	1.81	0.52	H
8.3	0.0270	50	7.20	3.55	0.83	0.42	E
10	0.0270	50	6.83	3.43	0.80	0.40	E
	0.0270	20	5.30	8.15	0.50	0.78	H
11.6	0.0270	50	7.33	3.26	0.75	0.36	E
13.3	0.0270	50	7.43	3.20	0.68	0.30	E
15	0.0270	20	6.00	7.95	0.66	1.28	H
	0.0270	20	6.96	7.79	0.64	0.75	E
	0.0270	50	5.40	2.98	0.51	0.38	H
	0.0270	50	6.71	3.60	0.55	0.38	H
16.6	0.0270	20	6.63	7.43	0.63	0.71	E
18.3	0.0270	20	6.35	7.08	0.71	0.69	E

f cps	2δ in.	S mv/cm	A cm	B cm	a cm	b cm	Rmks
20	0.0270	20	5.80	6.52	0.74	0.74	E
	0.0270	20	6.20	6.52	0.74	0.74	H
	0.0101	10	7.20	5.12	0.94	0.89	E
	0.0101	10	7.20	5.15	1.20	0.89	E
	0.0102	10	5.32	5.18	0.80	0.89	E
	0.0090	10	5.60	4.82	0.79	0.62	E
	0.0101	10	5.50	5.28	0.65	0.75	E
	0.0100	10	5.80	5.76	0.90	0.90	E
	0.0030	20	3.40	6.50	0.40	0.70	H*
	0.0028	20	7.60	6.20	1.10	0.80	H*
21	0.0102	10	5.20	5.00	0.79	0.91	E
21.6	0.0270	20	5.62	6.42	0.72	0.76	E
22	0.0102	10	5.10	4.92	0.73	0.70	E
23.3	0.0270	20	5.52	5.90	0.55	0.58	E
25	0.0270	20	5.10	5.78	0.57	0.66	E
26.6	0.0270	20	4.68	5.42	0.64	0.73	E
28.3	0.0270	20	6.40	6.04	0.72	1.06	H
	0.0270	20	4.82	6.44	0.44	0.70	E
	0.0270	20	7.40	6.42	0.81	0.88	H
30	0.0101	10	5.30	3.87	0.78	0.58	E
	0.0101	5	6.90	7.75	1.39	1.19	E
	0.0101	10	3.50	3.70	0.63	0.61	E
	0.0085	10	4.20	3.40	0.58	0.60	E
	0.0036	20	4.00	8.20	0.50	1.20	H*
	0.0033	20	7.60	8.00	1.20	1.10	H*
40	0.0090	10	4.40	3.21	0.60	0.72	E
	0.0101	5	5.80	6.30	1.01	1.03	E
	0.0090	10	3.40	3.39	0.60	0.50	E
	0.0078	10	3.50	2.93	0.58	0.41	E
	0.0039	20	4.20	9.00	0.72	1.37	H*
	0.0038	20	4.00	9.00	0.71	1.30	H*
50	0.0028	20	4.50	8.60	0.65	1.10	H*
	0.0034	20	4.40	9.20	0.78	1.50	H*
60	0.0081	5	3.05	4.19	0.45	0.80	E
	0.0081	5	5.90	4.20	0.90	0.62	E
	0.0082	5	5.38	4.64	0.95	0.81	E
	0.0068	5	2.42	4.00	0.44	0.62	E
	0.0095	5	7.09	5.82	1.40	0.98	E
	0.0035	50	5.60	4.10	1.10	0.75	H*
	0.0018	20	1.80	5.00		0.50	H*
70	0.0032	20	5.20	10.00	0.70	1.70	H*
	0.0016	10	4.40	9.90	0.85	1.90	H*
80	0.0069	2	4.20	8.61	0.71	1.20	E
	0.0069	2	6.01	8.58	0.89	1.18	E
	0.0073	5	4.60	3.60	0.80	0.60	E
	0.0060	5	2.00	3.32	0.38	0.50	E
	0.0081	2	5.80	9.21	1.00	1.60	E
	0.0014	20	5.60	5.40	1.30	0.82	H*
	0.0016	20	3.00	6.40	0.50	1.10	H*
100	0.0050	5	1.70	2.81	0.34	0.39	E
	0.0061	2	5.18	8.19	0.86	1.42	E
	0.0052	2	5.21	7.62	0.68	0.85	E
	0.0013	20	2.90	10.00	0.60	1.90	H*
	0.0012	50	5.90	4.00	1.30	0.90	H*

where f = Forcing frequency, cps.

2δ = Double amplitude of shear specimen, in.

S = Gain setting of oscilloscope, mv/cm.

H = Heiland amplifier w/filter used.

E = Ellis amplifier w/filter used.

H^* = Heiland amplifier w/o filter used.